NASA TECHNICAL MEMORANDUM

NASA TM X-3072

NASA TM X-3072

PLASMA TESTS OF SPRAYED COATINGS FOR ROCKET THRUST CHAMBERS

by Arthur N. Curren and Walter K. Love

Lewis Research Center
Cleveland, Ohio 44135

NATIONAL AERONAUTICS AND SPACE ADMINISTRATION • WASHINGTON, D. C. • JULY 1974

1. Report No.	2. Government Accession No.	3. Recipient's Catalog No.
NASA TM X-3072		

4. Title and Subtitle	5. Report Date
PLASMA TESTS OF SPRAYED COATINGS FOR ROCKET THRUST CHAMBERS	JULY 1974
	6. Performing Organization Code

7. Author(s)	8. Performing Organization Report No.
Arthur N. Curren and Walter K. Love	E-7877
	10. Work Unit No. 502-24
9. Performing Organization Name and Address Lewis Research Center National Aeronautics and Space Administration Cleveland, Ohio 44135	11. Contract or Grant No.
	13. Type of Report and Period Covered Technical Memorandum
12. Sponsoring Agency Name and Address National Aeronautics and Space Administration Washington, D.C. 20546	14. Sponsoring Agency Code

15. Supplementary Notes

16. Abstract

Several plasma-sprayed coating systems were evaluated for structural stability in hydrogen plasma and in oxygen plasma mixed with hydrogen plasma. The principal test heat flux was 24.5×10^{6} W/m^{2} (15 Btu/(in.^{2})(sec)). The system consisted of a number of thin (0.051×10^{-3} to 0.508×10^{-3} m (0.002 to 0.020 in.)) layers of metal oxides and/or metals. The principal materials included are molybdenum, nichrome, alumina, and zirconia. The study identifies important factors in coating system fabrication and describes the durability of the coating systems in the test environments. Values of effective thermal conductivity for some of the systems are indicated.

17. Key Words (Suggested by Author(s))
High-temperature coatings
Rocket engine heat transfer
Plasma-sprayed coatings

18. Distribution Statement
Unclassified - unlimited
Category 28

19. Security Classif. (of this report)	20. Security Classif. (of this page)	21. No. of Pages	22. Price*
Unclassified	Unclassified	53	$3.75

* For sale by the National Technical Information Service, Springfield, Virginia 22151

PLASMA TESTS OF SPRAYED COATINGS FOR ROCKET THRUST CHAMBERS

by Arthur N. Curren and Walter K. Love

Lewis Research Center

SUMMARY

Several plasma-sprayed coating systems were evaluated for structural stability in hydrogen plasma and in oxygen plasma mixed with hydrogen plasma. The principal test heat flux was 24.5×10^{6} W/m^{2} (15 Btu/(in.^{2})(sec)). The system consisted of a number of thin (0.051×10^{-3} to 0.508×10^{-3} m (0.002 to 0.020 in.)) layers of metal oxides and/or metals. The principal materials included are molybdenum, nichrome, alumina, and zirconia. The study identifies important factors in coating system fabrication and describes the durability of the coating systems in the test environments. Values of effective thermal conductivity for some of the systems are indicated.

INTRODUCTION

As mission and performance requirements for chemical and nuclear rocket engines become more ambitious, effective methods for augmenting thrust chamber cooling will become necessary. Attendant increases in heat flux and wall temperature levels approach or exceed regenerative cooling capabilities and limit chamber cyclic life. Several advanced hydrogen-oxygen engines concepts, including the space shuttle main engine, are currently close to this critical borderline and additional protection from stable thermal insulating coatings may be necessary. Reference 1 indicates that these coatings are also a potential solution for any potential nuclear rocket. If insulating material of suitable thickness is bonded to the hot gas side of the chamber wall, the heat flux through the wall and the metal interface temperature levels are reduced by virtue of the low thermal conductivity of the coating. Also, this reduction in heat flux is influenced by the coating material type and operating conditions.

The technology of coating techniques can include a wide variety of application methods. However, the only method evaluated in this investigation was plasma spraying of the various coatings. The advantages of plasma spraying include: (1) the process is relatively simple, (2) no special environmental chambers are required, (3) a wide range

of materials can be applied, and (4) process has the potential for field application and repair. Past experience has given indication that flame sprayed coatings cannot reliably withstand the continuous or cyclic environment within rocket thrust chambers. However, the failure modes and important variables involved in coatings have not been systematically explored in order to attain the potential advantages.

The purpose of this investigation was to examine a number of coating systems for their usefulness in chemical and nuclear rocket environments. Included in this study are simple coating systems consisting of a single thermal barrier applied over a suitable primer layer and more complex coating systems composed of more than one thermal barrier layer. Of particular interest is the "graded" coating system. Reference 2 describes the "graded" coating system concept and provides evidence of its superiority over a simple one-component coating from the standpoint of structural survivability during testing in a liquid oxygen - liquid ammonia rocket engine. A graded coating system is probably best described as a coating of metal and ceramic in which the composition is varied from a metal-rich mixture at the surface to be protected to a ceramic-rich mixture at the surface exposed to the hot gases. By this method, according to reference 2, the problem of weak, sensitive interfaces between metal and ceramic is reduced.

Most of the graded coating systems considered in this study are similar to those of reference 2, but with somewhat thinner sublayers. This structuring avoids relatively thick layers of any one composition and ideally allows for the control of relative thermal expansion between pairs of adjacent layers for the most severe imposed temperature gradient, so that critical shear stress levels are not exceeded. With some exceptions, the layers are so arranged that the material with the largest thermal expansion coefficient is adjacent to the thrust chamber metal wall, while the material with the lowest coefficient is exposed to the hot gas in the thrust chamber.

All of the graded coating systems included in this study were examined in an earlier preliminary screening effort and were reported in reference 3. In that work, numerous cooled, coated samples were exposed to an electric-arc plasma generator. The commercially fabricated coating systems of that study, however, lacked the thickness and composition controls necessary for a comprehensive comparative evaluation. It was apparent that the research group had to become personally familiar with the many parameters, their influences and trade-offs to impose more rigid controls on the coating application methods. Therefore, the coating systems for the current study were all fabricated at the Lewis Research Center. Great care was exercised in surface precoating preparation and the development of near-optimum coating equipment adjustments for each material and combination of materials applied. Additionally, premixed combinations of materials were "calibrated" so that the prescribed layer combinations of the most used mixtures were actually present in the final coating, in spite of the differences in plasma-sprayed deposition efficiencies of metals and ceramics. Determination of apparent near-

optimum material particle size for the spraying process was done as part of the mixture calibration effort.

For this investigation, eight different complex coating systems were applied to sample pieces which simulated sections of cooled rocket thrust chamber wall. An interesting variation of one of these basic systems was also examined, and six simple coatings were included for comparison. Three samples of each system were fabricated for a total of 45 coating samples for the program. The ingredients of the coating systems examined in this study were limited to selected metals and metal oxides. Included in these materials were molybdenum, nichrome, tungsten, alumina, zirconia, and chromia.

For each coating system, one sample was subjected to a maximum heat flux of 24.5×10^6 W/m^2 (15 Btu/(in.^{2})(sec)) for a maximum of 30 minutes accumulated time in the hydrogen environment and a second sample was similarly exposed to the hydrogen-oxygen environment. The third sample was reserved for possible later retesting to confirm results or for backup in case of an accident to one or two of the samples. These heat fluxes are representative of a level which can be dissipated by regenerative-cooling techniques. The exposure times are representative of real engine applications. The samples were tested with a relatively uniformly heated area of about 0.254 meter (1.0 in.) diameter. The heat was applied by means of a 200-watt (maximum) electric arc plasma generator which produced a hydrogen plasma plume in a low pressure (about 1.4×10^4 N/m^2 abs (2 psia)) environment. For simulation of a hydrogen-oxygen chemical rocket chamber environment, gaseous oxygen in a representative proportion was added to the hydrogen plasma plume.

The relative performances and individual structural changes of the coating systems were evaluated by means of direct observations, effective thermal conductivity determinations, microscopic section analysis, and X-ray diffraction techniques. The results of these observations are noted herein, along with some of the resulting implications for coating systems for actual thrust chamber applications.

This report displays all values in the International System of Units (SI) as the primary system. U.S. customary units also appear as a secondary system afterwards in parenthesis. The basic measurements and calculations for this study were made in U.S. customary units.

COATING SYSTEMS

The coating systems tested in this study were all designed and prepared at the Lewis Research Center. An in-house plasma-arc spraying facility was specifically set up to obtain controlled spray characteristics and repeatability of desired spray settings. The materials used were considered satisfactorily for thermal barrier systems in both reducing and in oxidizing environments. These materials included alumina, chromia,

hafnia, zirconia, and tungsten. Other materials were included for their anticipated value in enhancing component mixtures and oxide bonding to the substrate and for their expected influence on the thermal characteristics of mixtures with the oxides. These materials were nichrome, nickel, molybdenum, copper, and a gold brazing alloy. Tables I and II summarize the coating system materials and coating systems used in this study. Design and preparation of these coating systems was accomplished by evaluating the results from reference 3. The powders were prepared in-house and samples were coated by plasma arc spraying. Essentially, the calibrations to control coating system layer composition and thickness of the samples were accomplished by utilizing the information received from the in-house mixture preparation and power size determination.

APPARATUS AND EQUIPMENT

Sample Piece and Heat-Flux Meter

The design of the standard 304 stainless-steel test sample block is shown in figure 1(a). The standard block was coated with the various systems to be tested. Modifications to the standard block are also shown for the block used as a heat-flux meter. Both blocks had three brazed-in-place 347 stainless-steel tubes used for coolant flow passages and thermocouple instrumentation. Figure 1(b) indicates a typical cross-sectional area with a coating system applied. The center coolant tube receives the direct impact of the free plasma stream. The heat-flux meter test sample has two small diameter (0.254×10^{-3} m (0.010-in.)) thermocouple arrangements embedded in the tube wall with its sensing junction located at the tube crown. Figure 1(c) displays one such thermocouple junction and a more detailed description of the thermocouple assembly is shown in figure 2. Figure 3 indicates a typical photomicrographic cross-sectional area of the heat-flux-meter Chromel-Alumel thermocouple assembly.

Test Facility

The hot testing sequences were performed in a low altitude exhaust test chamber or containment vessel. Here, a plasma generator delivers the necessary heat flux energy levels to the coating system pieces. All components were contained in this closed vessel. Figure 4 is a schematic of the entire plasma generator test facility. Cooling of all components such as the plasma generator, heat-flux meter and coating system test pieces was accomplished by using distilled water to avoid foreign deposits on the internal surfaces. To facilitate various positions, angles, and distances during hot testing, an externally controlled positioning device was used in conjunction with the plasma

generator, test pieces, and heat-flux meters. The low pressure test chamber is shown in figure 5. This cutaway shows the orientation of the plasma generator, test piece, and heat-flux meter. A water cooled shield is used to protect the positioning device and instrument lines from heating damage during testing. This shield surrounds the test sample piece and the heat-flux meter to permit direct visual examination and closed circuit television monitoring through ports located at various places in the test chamber.

Plasma Generator

The plasma generator used in this study consists of an apparatus which utilizes partially ionized particles that are positively charged nuclei and electrons raised to high temperature by an electrical discharge. The temperature of the plasma depends upon the type and volume of gas used, the nozzle size, and amount of current. Figure 6 is a schematic of the apparatus used in this study.

For testing with hydrogen plasma, a stream of hydrogen gas is passed through an accelerating nozzle in which an electric arc (dc) charges the atom particles and raises them to a high temperature. This stream of hydrogen gas is continually being heated and compressed until it conducts electricity, and then a free plasma is generated out of the nozzle port area. The free plasma stream is pointed toward the test piece to be heated. From manufacturer's information, the plasma generator indicates free plasma temperatures of about 11 100 K (20 000° R). During operation of this plasma generator, the cables, fittings, and housing are protected by an integral water cooling system. Instrumentation at the nozzle entrance of this generator was not provided. Calculations indicated a hydrogen pressure of about 51.7×10^{-4} N/m^2 abs (75 psia) at the nozzle inlet condition.

From the previous investigation (figs. 7, 8, and 9 (ref. 3)), it was found that various factors controlled the amount of heat flux that was to be delivered to the coating system test piece. Some of these factors are the electrical input, hydrogen flow rate, distance of generator to sample, and nozzle condition. The dc power supply and plasma generator were estimated to have maximum power operating levels of about 200 kilowatts.

For testing with oxygen mixed with the hydrogen plasma, a three-port oxygen adapter was attached to the front end of the plasma generator (fig. 6). This permitted the desired hydrogen mixture ratio to be established adding gaseous oxygen in a representative proportion to the free hydrogen plasma. This type of oxygen injection was to simulate an oxidizing environment encountered in a hydrogen-oxygen chemical rocket chamber environment.

Instrumentation

The cooling water flow rates for the plasma generator, heat flux meter, and test sample were measured with turbine meters. The hydrogen, oxygen, purging nitrogen, and helium flow rates were measured by rotometers.

The heat-flux meter water pressure was separately measured by a Bourdon-tube gage, while the supply pressure was measured with an electrical transducer.

The coolant water temperature measurements for the plasma generator, heat-flux meter, and sample test pieces were measured by iron-constantan thermocouple assemblies.

For the alternating current supplied to the plasma generator, a variable transformer was used. Direct current supplied to the plasma generator was measured by a voltmeter.

EXPERIMENTAL PROCEDURES

Pretest Examinations

A standard procedure of examination (table II(a)) was applied to all of the coating system test pieces used in this investigation before and after testing. The methods used for the metallurgical processing were identical for all samples in order to make final evaluations and comparisons of the systems reliable. Tables are presented which summarize all the inspection results.

In most cases, two of the sample pieces of each coating were selected for 30-minute endurance testing; one in the reducing environment and the other in the oxidizing environment. The two selected samples were full-view color photographed for record of general appearances; closeup monochrome photographs at a magnification of three were made of the center testing area for the same purpose. In addition, visual microscopic examinations were made of the sample test area to take note of surface texture appearance, particle distribution, color, and other pertinent characteristics. Finally, coating system scrapings were taken from the tube end regions of the sample pieces for later crystal form comparison with scrapings taken from the central test zone of the samples. X-ray diffraction techniques were used for this comparison.

Cold-Shock Conditioning

All coating system samples were cold-shocked prior to hot testing. This simulates the rapid temperature drop from ambient to cryogenic temperature levels of a

regeneratively cooled thrust chamber wall. This cold-shock condition was accomplished by gravity filling the sample piece cooling tubes with liquid nitrogen (77.75 K (140° R)) at room temperature conditions. The sample piece was then allowed to return to ambient temperature room conditions. Next, a visual microscopic examination was made again of the sample test area. Results of all testing in liquid nitrogen indicated that no changes were noticed due to the cold-shock condition.

Hot Testing

The testing modes of the coating systems in this study consisted of two separate operations; hydrogen plasma environment and oxygen mixed with the hydrogen plasma. With hydrogen used as the working plasma gas in the plasma test facility, the reducing environment of a nuclear rocket was simulated. Seventeen of the 45 coated samples were tested with the hydrogen plasma at two different heat-flux levels. To simulate an oxidizing environment encountered in a chemical rocket, hydrogen with oxygen injection was used as the working plasma. These hydrogen-oxygen tests were performed on the sample pieces at a constant heat-flux level.

Prior to hot testing, all of the sample pieces and test environment were preconditioned. In the hydrogen tests, this conditioning consisted of purging the facility containment vessel with nitrogen and reducing the pressure to about 1.4×10^4 N/m^2 abs (2 psia). The purging with nitrogen was to prevent any combustion of the hydrogen plasma with oxygen in the vessel. This low pressure condition was maintained 15 minutes before hot testing to effectively purge the porous coating system structure of trapped air or moisture and to balance the pressure in any internal voids.

The testing consisted of 30 minutes of endurance tests and a 10-hour endurance test. The 30-minute endurance tests were conducted to determine the structural stability and bond strength of the coating systems under cyclic operation at high heat-flux levels. The test procedure consisted of a series of thermal cycles with a period between each cycle to visually examine the coating through the observation ports for the hydrogen plasma tests; each cycle consisted of a 2-minute exposure to a heat flux of 24.5×10^6 W/m^2 (15 Btu/(in.^{2})(sec)) followed by a 2-minute cooling and inspection time for a total of 15 cycles. For the oxygen-hydrogen plasma tests, the exposure time was 5 minutes per cycle for a total of six cycles. Seventeen of the sample pieces were tested at the heat-flux level of 24.5×10^6 W/m^2 (15 Btu/(in.^{2})(sec)) in the hydrogen environment. For comparison purposes, one sample piece was tested for 30 minutes at a heat-flux level of 19.6×10^6 W/m^2 (12 Btu/(in.^{2})(sec)) with the hydrogen plasma.

The purpose of the 10-hour exposure test was to determine the durability and structural integrity for long durations at a heat flux level comparable to a nuclear rocket of

16.3×10^6 W/m^2 (10 Btu/(in.^{2})(sec)). The coating system used for this test was selected on the basis of the results from reference 3. The test procedure consisted of 100 thermal cycles with a period between each cycle to visually examine the coating. Each cycle consisted of 6 minutes exposure to a heat flux of 16.3×10^6 W/m^2 (10 Btu/(in.^{2})(sec)) followed by a 2-minute cooling and inspection time.

General Operating Procedures

The test facility operating procedures for all phases of testing were similar except for the 10-hour duration test and the 30-minute test at 19.6×10^6 W/m^2 (12 Btu/(in.^{2})(sec)), which was the sample used for comparison purposes in regard to the phase one report. With regard to both testing environments (hydrogen and hydrogen-oxygen), the following paragraphs describes a standard procedure for the test facility operation.

Following the installation of the sample piece in the test facility, the pressure vessel was closed, sealed, and thoroughly purged with nitrogen to remove the enclosed air. Next, the tank was pressurized to about 20.7×10^4 N/m^2 abs (30 psia) with nitrogen. At this time, a leak check was monitored for 15 minutes. With no leakage encountered, the pressure vessel was reduced to about 1.4×10^4 N/m^2 abs (2 psia); this low pressure condition was maintained for 15 minutes to ensure a thorough coating system condition, as previously described.

Since the sample piece and heat flux meter are tied together for determining the heat flux through the coating system, the coolant supply weight flow rates and pressures were to be maintained at identical levels. Hence, the cooling water supply to the sample piece and heat-flux meter were each adjusted to 3.15 kilograms per second (6.94 lbm/sec or 50 gal/min) at 344.7×10^4 N/m^2 abs (500 psia). The other components which required water for cooling were also adjusted to their proper values. Alinement of the plasma generator on the heat-flux meter instrumentation followed with the spacing of the generator nozzle exit to the heat-flux meter. This distance was 8.89×10^{-2} meter (3.5 in.). The plasma gas weight flow rate through the plasma generator was adjusted to a specific flow rate in which the generator was started by means of a high frequency current pulse to establish an arc. Then, with the plasma stream impinging on the heat-flux meter, the electrical power to the generator was adjusted to produce the desired heat-flux level. When the desired heat-flux level was obtained, the coating system sample piece was moved into the plasma stream to replace the heat-flux meter and the cyclic testing sequence was conducted with constant electrical power and the working gas flow rate settings. Upon termination of the test operation, the heat-flux meter was again moved into the plasma stream to replace the sample piece and recheck the heat-flux level. Then the electrical power was reduced to zero.

RESULTS AND DISCUSSION

The coating systems considered in this study may be conveniently placed in four general groupings. Where a single oxide (containing only small amounts of other materials such as stabilizers) is the primary or outer thermal insulator and is applied directly over a single-adhesive layer coating, the coating system may be described as a simple one. This description includes systems 017, 018, 019, 021, 022, and 023 which are detailed in table I. Where the primary single-component oxide insulator is applied over two or more sublayers of single-component material, the system may be described as layered. This description includes systems 004 and 005. A simple-graded coating system is one in which one or more layers containing mixtures of a single metal and a single oxide are applied to an adhesive layer to provide adhesion of the oxide to the tube wall. This coating system type is characterized by having an outer primary insulating layer of a single material and includes systems 001, 003, and 007. Finally, coating systems that utilize more than one component material in the outer thermal insulator layer and/or are applied over a substructure wherein the binder layer consists of more than two component materials and the intermediate layers consist of more than two component materials are herein termed compound-graded systems. Included in this last group are systems 002, 006, 008, and 020. This nomenclature will be used throughout the remainder of this report.

One specimen from each coating system was subjected to a series of 2-minute exposures to an accumulated total of 30 minutes in a heat flux of 24.5×10^6 W/m^2 (15 Btu/(in.^{2})(sec)) in hydrogen plasma in the test facility. For most of the samples, the heat flux was increased gradually during the first minute of exposure through a series of brief steady state levels and the observed surface temperature at each of these levels was noted. This information was to provide data for the determination of overall effective coating system thermal conductivity. Fresh specimens of each coating system were then subjected to a series of 5-minute exposures to an accumulated total of 30 minutes in a heat flux of 24.5×10^6 W/m^2 (15 Btu/(in.^{2})(sec)) in oxygen mixed with hydrogen plasma. The oxygen-to-hydrogen mixture ratio by weight was very near 5.5 to 1.0. The third sample in this case was subjected to a heat flux of 16.3×10^6 W/m^2 (10 Btu/(in.^{2})(sec)) for a total of 10 hours in hydrogen plasma. Each specimen was examined visually and by X-ray diffraction before and after testing. Metallographic cross sections of one end of the sample and of the central, tested portion of the sample were also made and studied. The results of the examinations are presented in the following sections. The section photomicrographs of the coolant tube end regions will be identified as "untested" while those of the tested area will be identified as "tested" where they appear in the figures.

In considering the test results, it should be noted that the general testing procedure employed - common heat flux testing for all the coating systems - probably resulted in a different surface temperature for each system. Coating systems with high thermal resistances had higher surface temperatures than systems with lower thermal resistance

for the same heat flux. Therefore, some of the surface effects noted in the tested samples may have been influenced by this temperature nonuniformity. Further, because of the relatively low gas weight flow rate used in the tests, coating system surface features in the tested samples may be different from those exposed to the same heat flux for the same period of time in an actual rocket thrust chamber. In an actual chamber, the more loosely attached coating system fragments would probably be blown away, while in the plasma tests they remain. For this reason, the before and after testing coating system thickness measurements shown in table I should not be used as a measure of the relative survivability of the coatings by themselves. Several of the tested coating systems apparently survived the test sequences quite well with almost no thickness loss, but flaked and fell from the sample test piece readily when they were gently abraded with a smooth instrument. Quite clearly, then, these coating systems would not have survived the environment of a rocket thrust chamber. In spite of this difficulty, however, from the standpoint of having most of the coating material present for examination after testing, the plasma tests have a decided advantage over actual chamber tests for materials selection and/or coating screening studies.

Simple Coating Systems

All the simple coating systems, types 017, 018, 019, 021, 022, and 023 have common, relatively thin 0.051×10^{-3}-meter (0.002-in.) binder or base coatings of molybdenum (Mo). The substrates, or protected surfaces, for these samples and all other samples in this study, were all grit-blasted to an average surface roughness of 3.175 rms micrometers (125 rms μin.). Systems 017, 018, and 019 had a relatively thick 0.254×10^{-3}-meter (0.010-in.) primary insulating layers of aluminum oxide (Al_2O_3, or alumina), zirconium oxide (ZrO_2, or zirconia) stabilized with calcium oxide (CaO, or calcia), and zirconia stabilized with yttrium oxide (Y_2O_3, or yttria), respectively. Coating systems 021, 022, and 023 were the material counterparts of systems 017, 018, and 019, respectively, but having relatively thin primary insulator layer thicknesses of 0.127×10^{-3} meter (0.005 in.). All the yttria-stabilized-zirconia coating material used in this study was prepared by means of sintering and pulverizing before spraying. In all discussions relating to these materials in later portions of this report, calcia-stabilized zirconia will be denoted as $ZrO_2 \cdot CaO$.

For reference, pure zirconia at room temperature is monoclinic in crystal form and reversibly transforms to a tetragonal form near 1366 K (2460° R). Accompanying the phase change is a rather abrupt, crack-promoting density increase of about 8 percent. When calcia or yttria is added to zirconia in solid solution, the zirconia becomes partially or fully stabilized, depending on the relative amount of the additive. Stabilized

zirconia is cubic crystalline in form and retains that form to its melting temperature. Stabilized zirconia is characterized by uniform thermal expansion characteristics.

The first results to be described are those concerning the relative survivability of a coating system having a relatively thin primary coating of Al_2O_3 in the two environments considered in this study. Figure 15 shows views of samples 021-1-c and 021-2-c after testing. While neither sample was severely damaged, the measurements indicated in table I show that the primary coating thickness reduction was greatest in the hydrogen plasma test. Table III(a) indicates visual and X-ray diffraction results of the samples.

In a similar test involving the relative survivability of coating system 022-1-c and 022-2-c with a relatively thin $ZrO_2 \cdot CaO$ primary coating, figure 16 shows the 022-1-c coating suffered less loss in the hydrogen plasma test.

Simple coating systems having relatively thick primary layers of Al_2O_3 (017-1-c) or $ZrO_2 \cdot CaO$ (018-3-c) did not perform well at all and were literally destroyed by their inability to support internal thermal stress gradients. Figure 17(a-1) and (a-2) shows their post-test appearance after essentially identical test cycles. It appears that applying relatively thick ceramic coatings to rocket thrust chambers in order to achieve a required high thermal resistance can, in fact, hasten the destruction of the coating system.

The use of Y_2O_3 to stabilize ZrO_2 does not appear to yield better results than does the use of CaO. Figure 17(b-1) shows a sample (019-1-c) which had a relatively thick primary layer of $ZrO_2 \cdot Y_2O_3$ and was subjected to the standard 30-minute test cycle in hydrogen plasma. While its appearance is somewhat different than the sample in figure 17(a-2) (018-3-c), which was a similarly tested $ZrO_2 \cdot CaO$ sample, the results are the same. In both cases, the primary layer was completely removed from the sample. Figure 17(b-2) shows a sample (023-1-c) with a relatively thin $ZrO_2 \cdot Y_2O_3$ primary coating after the same hydrogen plasma test cycle. This sample does not appear to have resisted damage quite as well as similarly tested sample 022-1-c shown in figure 16(a-1) and (a-2) that had a relatively thin primary layer of $ZrO_2 \cdot CaO$.

The measured overall effective thermal conductivity values for the six simple coating system types tested are shown in figure 10 and table IV(a).

Layered Coating Systems

Only two layered coating system types were in the samples included in this study. Both coating system types 004 and 005 were characterized by having relatively thin 0.051×10^{-3}-meter (0.002-in.) base coatings of molybdenum. On this base coating, both sample types had somewhat thicker (0.0762×10^{-3} m or 0.003 in. design) coating of nichrome. System type 004 had a primary coating of 0.1016×10^{-3}-meter (0.004-in.) Al_2O_3, while system type 005 had a similar 0.1016×10^{-3}-meter (0.004-in.) primary coating of $ZrO_2 \cdot CaO$.

System type 005 having $ZrO_2 \cdot CaO$ as the primary layer demonstrated much better survivability than did system type 004 which utilized Al_2O_3 in that capacity. Reference to table I readily indicates the primary layer thickness loss of system type 005 is much less than that of type 004. While neither system type was catastrophically damaged (gross spalling, cracking, etc.) during the test procedures, the Al_2O_3 primary layers in both samples 004-2-c and 004-3-c were essentially completely removed. The $ZrO_2 \cdot CaO$ primary layer in system type 005, on the other hand, was reduced only slightly in thickness during testing in either test environment. If a layered coating system is to be employed in this type of application, then, clearly, a primary layer of $ZrO_2 \cdot CaO$ is to be preferred over one of Al_2O_3. Figure 18(a) shows the effect on sample 005-1-c of testing in the hydrogen plasma; while figure 18(b) shows sample 004-2-c after testing in the hydrogen-oxygen environment.

As was reported in reference 3, coating layers of Al_2O_3 and Al_2O_3-rich material exhibit markedly different change characteristics during exposure to the test environment than do layers of $ZrO_2 \cdot CaO$ and $ZrO_2 \cdot CaO$-rich material. In general, the Al_2O_3-based layers characteristically displayed shrinkage and apparent particle-by-particle erosion with no significant evidence of cracking or spalling. The $ZrO_2 \cdot CaO$-based layers, on the other hand, characteristically displayed closely patterned deep cracks and lost material in relatively large pieces at locations where cracks intersected, particularly beneath the surface. These visual observations are corroborated for the Al_2O_3 case by the X-ray diffractive results indicated in table III(b). In many cases, the stable (alpha) form of the material was more in evidence than the unstable (gamma) form after testing than before indicating this form was probably reverting to the stable form during testing. (The unstable forms were probably produced by the extremely rapid quenching rates characteristic of the plasma-spray application technique. The phase change to the stable alpha form is accompanied by a density increase of from 3.60×10^3 kg/m^3 (0.13 lb/in.^{3}) for the gamma phase to 3.96×10^3 kg/m^3 (0.143 lb/in.^{3}) for the alpha phase. Thus, during exposure, there can be a shrinkage of the coating up to 10 percent. While the X-ray diffraction studies do not clearly reveal the reason for the cracks in the $ZrO_2 \cdot CaO$-based layers, it may be speculated that local destabilization occurs, creating a favorable situation for cracking. It should be pointed out that one system sample (022-2-c) shows some unstable monoclinic ZrO_2 after testing where only the cubic form was in evidence prior to testing.

Overall effective thermal conductivity measurements were only made for system type 005, and these are indicated in figure 11 and table IV(b). Again, except for values of coating mean temperature below about 1100 K (1900° R) they were very near the referenced value for bulk ZrO_2.

Simple-Graded Coating Systems

Coating system types 001, 003, and 007 are the simple-graded coating systems examined in this study. Types 001 and 003 have thin 0.051×10^{-3}-meter (0.002-in.) molybdenum base layers, while type 007 has a similarly thin nichrome base coating. On the base coating, type 001 has three thin 0.051×10^{-3}-meter (0.002-in.) graded layers of nichrome and $ZrO_2 \cdot CaO$ mixtures which underlie the primary $ZrO_2 \cdot CaO$ layer which is 0.1016×10^{-3} meter (0.004 in.). The relative $ZrO_2 \cdot CaO$ content of the graded layers increase from 30 through 70 to 90 percent by weight as they are applied. Details of these coating systems are noted in table I.

Coating system type 003 has a similarly graded series of three sublayers composed of nichrome and Al_2O_3 on which is deposited a primary coating of thin 0.1016×10^{-3}-meter (0.004-in.) Al_2O_3.

A "hybrid" coating system is represented by coating system 007. On a thin 0.051×10^{-3}-meter (0.002-in.) nichrome base coating is deposited two 0.076×10^{-3}-meter (0.003-in.) graded layers of nichrome and Al_2O_3. The primary coating is a thicker 0.1016×10^{-3}-meter (0.004-in.) layer of $ZrO_2 \cdot CaO$.

Of the three coating types, 003 suffered the most primary coating loss. This is indicated by the measurements noted in table I. The reason for this may have been that the exterior surface temperature reached values close to melting for Al_2O_3 and accelerated material erosion. It should be noted the most primary coating material loss was displayed by sample 003-2-c, which had a considerably thicker system than sample 003-1-c, and which would have had a resulting higher surface temperature for the same heat flux level. Because of this temperature difference, it is not clear whether the coating type performed best in the hydrogen or the hydrogen-oxygen environment.

Coating system types 001 and 007 performed quite well, about equally, in both test environments. Material loss was quite small in all the tests on these samples. Figure 19 shows photomicrographs of the sample 001-1-c before and after testing. In addition to the typical crack pattern characteristics of $ZrO_2 \cdot CaO$ and $ZrO_2 \cdot Y_2O_3$ coatings, this figure shows a void pattern in the post-test sample which suggests some sublayer metal component (nichrome) melting.

The tests on sample type 007 were probably the most revealing in the test series to this point. Examination of the photographs of figure 20 indicates that the crack pattern in the primary $ZrO_2 \cdot CaO$ layers extend to, but do not penetrate the sublayers, which are Al_2O_3-based mixtures. Further, the $ZrO_2 \cdot CaO$ primary layer remained well bonded with the sublayers and did not become detached even with vigorous abrasion with a dull instrument. The implications of this test are that the high temperature capability of a primary $ZrO_2 \cdot CaO$ layer coupled with the crack resisting characteristics of an Al_2O_3-based underlayer structure may provide the basis for a highly successful coating system for environments and heat-flux levels in the range of this study.

The measured overall effective thermal conductivity values for the three simple-graded coating systems are shown in figure 12 and table IV(c). Predictably, the Al_2O_3 bearing coating systems have thermal conductivity values somewhat higher than those of the $ZrO_2 \cdot CaO$-based system. However, the values or conductivity for these simple-graded systems are, again, nominally the same as bulk zirconia.

Since the test vessel was routinely purged with N_2 (nitrogen) before testing, some residual N_2 remained in the test environment. Examination of table III(c) shows post-test X-ray diffraction tests of the $ZrO_2 \cdot CaO$ and $ZrO_2 \cdot Y_2O_2$ samples typically indicate the presence of cubic ZrN (zirconium nitride). To examine the effect of this material on the test results, a fresh sample, 001-3-c was tested in the hydrogen plasma environment after repeatedly purging the test vessel with the helium (He). Post-test X-ray diffraction tests, as expected, did not indicate the presence of even trace quantities of ZrN. The photomicrographic studies of this sample revealed no identifiable differences in appearance, material loss, or coating adherence to the sublayer structure. It was, therefore, concluded that the formation of the small quantities of ZrN during the test procedure did not confuse or affect the overall test results. The general use of He for purging the test vessel was precluded because of cost and availability considerations.

Compound-Graded Coating Systems

Coating systems type 002, 020, 006, and 008 were the compound-graded coating systems included in this study. Types 002 and 020 were quite similar in that the 0.051×10^{-3}-meter (0.002-in.) base layer was coated with graded 0.051×10^{-3}-meter (0.002-in.) thick sublayers. These sublayers were molybdenum and ZrO_2 graded from 17.42 to 65.49 percent ZrO_2 by weight. The primary layers were composed of HfO_2 (hafnium oxides or hafnia) and ZrO_2, in the relative quantities indicated in table I. The basic difference between the two coating systems was the stabilization material used with the ZrO_2. In coating system type 002, CaO was used, while type 020 used Y_2O_3.

In the standardized test cycles in the two environments of this study, coating system types 002 and 020 performed similarly. The characteristic ZrO_2 surface cracking patterns occurred in both types, but both surfaces remained well attached and did not readily fall off when subjected to post-test abrasion. The cross-section photomicrographs of sample 002-2-c and 020-2-c shown in figure 21 indicate a more homogeneous material particle distribution in sample 020-2-c, but apparently this had no significant effect on performance. It must be concluded than that any improvement in performance in this application due to the use of Y_2O_3 rather than CaO as a ZrO_2 stabilizing agent is not significant and does not justify the higher cost of the Y_2O_3.

Following these tests, a fresh sample (002-3-c) of system type 002 was subjected to a 10-hour (total lapsed time) test in hydrogen plasma 16.3×10^6 W/m^2 (10 Btu/(in.^{2})(sec)).

This heat-flux level was selected as a level compatible with long term usage of the test equipment. Comparative views of sample 002-1-c, run for 30 minutes in hydrogen plasma, and sample 002-3-c, run for 10 hours in hydrogen plasma, appear in figure 22. While sample 002-1-c displayed typical cracks, the 10-hour sample 002-3-c displayed far more extensive deep, wide cracks. The surface of this sample failed readily when abraded, and some pieces of material which fell away extended to the sample substrate surface. Obviously, this coating system would not be successful in this application.

Figure 23 shows post-test surface view of coating system types 006 and 008, whose construction details are indicated in table I. Type 006 is a relatively thick 0.6096×10^{-3}-meter (0.024-in.) tungsten (W)-chromium (Cr)-based system, and type 008 is a thinner 0.3049×10^{-3}-meter (0.012-in.) Cr-chromia (CrO_2)-based system. Both systems exhibited only very minor thickness loss during the testing procedure; but after testing, the coating material in the test area crumbled and fell from these samples when they were lightly brushed with a dull instrument. Again, these coatings must be considered most useful for this application from the results of these tests. Table III(d) indicates visual and X-ray diffraction results of the samples.

Measured overall effective thermal conductivity values for these compound-graded coating systems are shown in figures 13 and 14 and table IV(d).

SUMMARY OF RESULTS

Several plasma-sprayed coating systems were fabricated and tested with hydrogen plasma and with oxygen mixed with hydrogen plasma to determine their usefulness in a chemical and nuclear rocket application. The standard testing cycle was for an accumulated time period of 30 minutes at a heat flux of 24.5×10^6 W/m^2 (15 Btu/(in.^{2})(sec)). One sample was tested for a total time of 10 hours at 16.3×10^6 W/m^2 (10 Btu/(in.^{2})(sec)) in hydrogen plasma. The effective thermal conductivity of most of the coating systems was determined during the testing in hydrogen plasma. Each sample was examined before and after testing by visual and X-ray diffraction techniques. The coating systems were evaluated and compared after testing. The results which are summarized in the following statements are restricted to the testing conditions described and may not be valid in test conditions which are significantly different.

1. A uniform, relatively homogeneous prescribed ceramic-metal coating mixture can be applied to a suitable substrate by means of commercially available single-nozzle plasma spray equipment. This can be accomplished by premixing the powder from components in controlled, calibrated mixtures and particle sizes.

2. Measurements indicate the effective thermal conductivity values for the coating systems evaluated in this study are significantly lower than those which would be calculated for the systems using any of a number of commonly accepted bulk property

weighting mixture methods. In addition, it should be noted that all the measured ues, regardless of material, over the test temperature range are quite near the referenced value for bulk zirconia.

3. In testing the simple coating systems in this study, it developed clearly that relatively thin ceramic layers retain their structural integrity (resisted spalling and cracking) far better than thicker ones. In later testing, it became equally clear that this characteristic extended to the outer ceramic layers in more complex coating systems.

4. The aluminum oxide (Al_2O_3) and alumina-metal mixture coating system layers tested in this study characteristically displayed shrinkage due to phase change and particle-by-particle erosion with no significant cracking. The zirconia (ZrO_2) and zirconia-metal mixtures, however, characteristically developed close-patterned deep cracks regardless of the stabilized method and lost material in relatively large pieces in those locations where the cracks intersected.

5. The relatively thin zirconia-based simple coating system performed better from a structural stability standpoint in the hydrogen plasma tests than did the counterpart alumina-based system. Conversely, the thin alumina-based simple coating system demonstrated performance in the oxygen-mixed-with-hydrogen plasma environment superior to that of the zirconia-based system. Extension of these characteristics to the more complex coating systems is not clearly evident.

6. The addition of a single additional one-component nichrome sublayer to the simple coating system thereby forming a layered coating system consistently resulted in improved structural performance in the tests conducted in this study. This very simple modification could be significant in an application where a simple coating system demonstrates only marginal performance.

7. The structural performance of the two zirconia-based compound-graded coating systems tested which differed only in the method of zirconia stabilization (types 002 and 020) was essentially identical. Therefore, from these results, neither stabilization by calcia (CaO) or yttria (Y_2O_3) can be preferred over the other.

8. The nichrome-alumina-zirconia based simple-graded coating system (type 007) and the two equivalent zirconia-based compound-graded coating systems (types 002 and 020 performed best and equally well structurally in the 30-minute endurance tests in this study. All the samples displayed characteristic zirconia surface cracking, but with little material loss. While the cracks in the compound-graded coating system extended into the sublayers, the cracks in the simple-graded coating system terminated at the nichrome-alumina sublayer level. This apparent crack-terminating property of an alumina-rich sublayer implies possible application in advanced coating systems.

9. The zirconia-based compound-graded coating system (type 002) which was tested in hydrogen plasma for 10 hours exhibited unacceptable structural characteristics after testing. The coating was deeply cracked in a fine pattern and became detached from the

substrate with very slight surface abrasion. It seems evident that with the surface shear at the rocket thrust chamber wall, the bulk of the coating would have been removed during testing.

Lewis Research Center,
National Aeronautics and Space Administration,
Cleveland, Ohio, March 20, 1974,
502-24.

REFERENCES

1. Robbins, William H.; Bachkin, Daniel; and Medeiros, Arthur A.: An Analysis of Nuclear-Rocket Nozzle Cooling. NASA TN D-482, 1960.
2. Hjelm, Lawrence N.; and Bornhorst, Bernard R.: Development of Improved Ceramic Coatings to Increase the Life of XLR99 Thrust Chamber. Research-Airplane-Committee Report on Conference on the Progress of the X-15 Project. NASA TM X-57072, 1961, pp. 227-253.
3. Curren, Arthur N.; Grisaffe, Salvatore J.; and Wycoff, Kurt C.: Hydrogen Plasma Tests of Some Insulating Coating Systems for the Nuclear Rocket Thrust Chamber. NASA TM X-2461, 1972.
4. Touloukian, Y. S., ed.: Thermalphysical Properties of High Temperature Solid Materials. Macmillan Co., 1967.
5. Schacht, Ralph L.; Price, Harold G., Jr.; and Quentmeyer Richard J.: Effective Thermal Conductivities of Four Metal-Ceramic Composite Coatings in Hydrogen-Oxygen Rocket Firings. NASA TN D-7055, 1972.

TABLE I. - SUMMARY OF SPECIFICATIONS OF COATING SYSTEMS EVALUATED

(a) Simple coating systems

Sample	Design specifications				Test cycle	Pretesting thickness		Post-testing thickness	
	Layer	Material, percent by weight	Thickness			mm	in.	mm	in.
			mm	in.					
017-1-c	1	Molybdenum	0.0508	0.0020	(a)	0.0091	0.0039	0.0635	0.0025
	2	Alumina	.2540	.0100		.2184	.0086	.0177	.0007
		Total	0.3048	0.0120		0.3175	0.0125	0.0812	0.0032
017-2-c	1	Molybdenum	0.0508	0.0020	(b)	0.0685	0.0027	0.0813	0.0032
	2	Alumina	.2540	.0100		.4115	.0162	------	------
		Total	0.3048	0.0120		0.4800	0.0189	0.0813	0.0032
018-3-c	1	Molybdenum	0.0508	0.0020	(a)	0.0533	0.0021	0.1245	0.0049
	2	Zirconia (CaO)	.2540	.0100		.2845	.0112	------	------
		Total	0.3048	0.0120		0.3378	0.0133	0.1245	0.0049
018-2-c	1	Molybdenum	0.0508	0.0020	(b)	0.0533	0.0021	0.0406	0.0016
	2	Zirconia (CaO)	.2540	.0100		.3378	.0133	.0229	.0009
		Total	0.3048	0.0120		0.3911	0.0154	0.0635	0.0025
019-3-c	1	Molybdenum	0.0508	0.0020	(a)	0.0787	0.0031	0.0686	0.0027
	2	Zirconia (Y_2O_3)	.2540	.0100		.2007	.0079	------	------
		Total	0.3048	0.0120		0.2794	0.0110	0.0686	0.0027
019-2-c	1	Molybdenum	0.0508	0.0020	(b)	0.0584	0.0023	0.0737	0.0029
	2	Zirconia (Y_2O_3)	.2540	.0100		.1981	.0078	.1422	.0056
		Total	0.3048	0.0120		0.2565	0.0101	0.2159	0.0085
021-1-c	1	Molybdenum	0.0508	0.0020	(a)	0.0584	0.0023	0.0127	0.0005
	2	Alumina	.1270	.0050		.1524	.0060	.0228	.0009
		Total	0.1778	0.0070		0.2108	0.0083	0.0356	0.0014
021-2-c	1	Molybdenum	0.0508	0.0020	(b)	0.0559	0.0022	0.0406	0.0016
	2	Alumina	.1270	.0050		.2209	.0087	.0864	.0034
		Total	0.1778	0.0070		0.2768	0.0109	0.1270	0.0050
022-1-c	1	Molybdenum	0.0508	0.0020	(a)	0.0635	0.0025	0.0660	0.0026
	2	Zirconia (CaO)	.1270	.0050		.1092	.0043	.0940	.0037
		Total	0.1778	0.0070		0.1727	0.0068	0.1600	0.0063
022-2-c	1	Molybdenum	0.0508	0.0020	(b)	0.0432	0.0017	0.0483	0.0019
	2	Zirconia (CaO)	.1270	.0050		.1193	.0047	.0914	.0036
		Total	0.1778	0.0070		0.1625	0.0064	0.1397	0.0055
023-1-c	1	Molybdenum	0.0508	0.0020	(a)	0.0991	0.0039	0.0813	0.0032
	2	Zirconia (Y_2O_3)	.1270	.0050		.0838	.0033	.0228	.0009
		Total	0.1778	0.0070		0.1829	0.0072	0.1041	0.0041
023-2-c	1	Molybdenum	0.0508	0.0020	(b)	0.0635	0.0025	0.0584	0.0023
	2	Zirconia (Y_2O_3)	.1270	.0050		.1498	.0059	------	------
		Total	0.1778	0.0070		0.2133	0.0084	0.0584	0.0023

[a] H_2 environment at 24.5×10^6 W/m^2 (15 Btu/(in.^{2})(sec)) in 2-minute cycles for a total time of 30 minutes duration.

[b] H_2-O_2 environment at 24.5×10^6 W/m^2 (15 Btu/(in.^{2})(sec)) in 5-minute cycles for a total time of 30 minutes duration.

TABLE I. - Continued. SUMMARY OF SPECIFICATIONS OF COATING SYSTEMS EVALUATED

(b) Layered coating systems

Sample	Design specifications				Test cycle	Pretesting thickness		Post-testing thickness	
	Layer	Material, percent by weight	Thickness			mm	in.	mm	in.
			mm	in.					
004-3-c	1	Molybdenum	0.0508	0.0020	(a)	0.0483	0.0019	0.0533	0.0021
	2	Nichrome	.0762	.0030		.0610	.0024	.1651	.0065
	3	Alumina	.1016	.0040		.1422	.0056	------	------
		Total	0.2286	0.0090		0.2515	0.0099	0.2184	0.0086
004-2-c	1	Molybdenum	0.0508	0.0020	(b)	0.0762	0.0030	0.0660	0.0026
	2	Nichrome	.0762	.0030		.0686	.0027	.0966	.0038
	3	Alumina	.1016	.0040		.1905	.0075	.0406	.0016
		Total	0.2286	0.0090		0.3353	0.0132	0.2032	0.0080
005-1-c	1	Molybdenum	0.0508	0.0020	(a)	0.0686	0.0027	0.0787	0.0031
	2	Nichrome	.0762	.0030		.0559	.0022	.0432	.0017
	3	Zirconia (CaO)	.1016	.0040		.1422	.0056	.1168	.0046
		Total	0.2286	0.0090		0.2667	0.0105	0.2387	0.0094
005-2-c	1	Molybdenum	0.0508	0.0020	(b)	0.0483	0.0019	0.0635	0.0025
	2	Nichrome	.0762	.0030		.0813	.0032	.0610	.0024
	3	Zirconia (CaO)	.1016	.0040		.1397	.0055	.1422	.0056
		Total	0.2286	0.0090		0.2693	0.0106	0.2667	0.0105

[a] H_2 environment at 24.5×10^6 W/m^2 (15 Btu/(in.^{2})(sec)) in 2-minute cycles for a total time of 30 minutes duration.

[b] H_2-O_2 environment at 24.6×10^6 W/m^2 (15 Btu/(in.^{2})(sec)) in 5-minute cycles for a total time of 30 minutes duration.

TABLE I. - Continued. SUMMARY OF SPECIFICATIONS OF COATING SYSTEMS EVALUATED

(c) Simple-graded coating systems

Sample	Design specifications				Test cycle	Pretesting thickness		Post-testing thickness	
	Layer	Material, percent by weight	Thickness			mm	in.	mm	in.
			mm	in.					
003-1-c	1	Molybdenum	0.0508	0.0020	(a)	0.0406	0.0016	0.0381	0.0015
	2	70Nichrome-30Al_2O_3	.0508	.0020		.0889	.0035	.1448	.0057
	3	30Nichrome-70Al_2O_3	.0508	.0020		------	------	------	------
	4	10Nichrome-90Al_2O_3	.0508	.0020		------	------	------	------
	5	Alumina	.1016	.0040		.2007	.0079	.0889	.0035
		Total	0.3048	0.0120		0.3302	0.0130	0.2718	0.0107
003-2-c	1	Molybdenum	0.0508	0.0020	(b)	0.0457	0.0018	0.0406	0.0016
	2	70Nichrome-30Al_2O_3	.0508	.0020		.2388	.0094	.0356	.0014
	3	30Nichrome-70Al_2O_3	.0508	.0020		------	------	.1270	.0050
	4	10Nichrome-90Al_2O_3	.0508	.0020		------	------	------	------
	5	Alumina	.1016	.0040		.1625	.0064	.0381	.0015
		Total	0.3048	0.0120		0.4470	0.0176	0.2413	0.0095
007-1-c	1	Nichrome	0.0508	0.0020	(a)	0.0406	0.0016	0.0584	0.0023
	2	50Nichrome-50Al_2O_3	.0762	.0030		.1930	.0076	.1905	.0075
	3	20Nichrome-80Al_2O_3	.0762	.0030		------	------	------	------
	4	Zirconia (CaO)	.1016	.0040		.1397	.0055	.1473	.0058
		Total	0.3048	0.0120		0.3733	0.0147	0.3962	0.0156
007-2-c	1	Nichrome	0.0508	0.0020	(b)	0.0457	0.0018	0.0635	0.0025
	2	50Nichrome-50Al_2O_3	.0762	.0030		.1651	.0065	.1499	.0050
	3	20Nichrome-80Al_2O_3	.0762	.0030		------	------	------	------
	4	Zirconia	.1016	.0040		.1905	.0075	.1244	.0049
		Total	0.3048	0.0120		0.4013	0.0158	0.3378	0.0133
001-1-c	1	Molybdenum	0.0508	0.0020	(a)	0.0762	0.0030	0.0584	0.0023
	2	70Nichrome-30ZrO_2	.0508	.0020		.1118	.0044	.0483	.0019
	3	30Nichrome-70ZrO_2	.0508	.0020		------	------	------	------
	4	10Nichrome-90ZrO_2	.0508	.0020		------	------	------	------
	5	Zirconia (CaO)	.1016	.0040		.1453	.0058	.1625	.0064
		Total	0.3048	0.0120		0.3353	0.0132	0.2692	0.0106
001-2-c	1	Molybdenum	0.0508	0.0020	(b)	0.0737	0.0029	0.0381	0.0015
	2	70Nichrome-30ZrO_2	.0508	.0020		.1625	.0064	.1575	.0062
	3	30Nichrome-70ZrO_2	.0508	.0020		------	------	------	------
	4	10Nichrome-90ZrO_2	.0508	.0020		------	------	------	------
	5	Zirconia (CaO)	.1016	.0040		.1321	.0052	.1575	.0062
		Total	0.3048	0.0120		0.3683	0.0145	0.3531	0.0139
001-3-c	1	Molybdenum	0.0508	0.0020	(c)	0.0406	0.0016	0.0305	0.0012
	2	70Nichrome-30ZrO_2	.0508	.0020		.1422	.0056	.1270	.0050
	3	30Nichrome-70ZrO_2	.0508	.0020		------	------	------	------
	4	10Nichrome-90ZrO_2	.0508	.0020		------	------	------	------
	5	Zirconia (CaO)	.1016	.0040		.1016	.0040	.0914	.0036
		Total	0.3048	0.0120		0.2844	0.0112	0.2489	0.0098

[a] H_2 environment at 24.5×10^6 W/m^2 (15 Btu/(in.^{2})(sec)) in 2-minute cycles for a total time of 30 minutes duration.

[b] H_2-O_2 environment at 24.5×10^6 W/m^2 (15 Btu/(in.^{2})(sec)) in 5-minute cycles for a total time of 30 minutes duration.

[c] Helium environmental purge.

TABLE I. - Concluded. SUMMARY OF SPECIFICATIONS OF COATING SYSTEMS EVALUATED

(d) Compound-graded coating systems

Sample	Design specifications				Test cycle	Pretesting thickness		Post-testing thickness	
	Laye	Material, percent by weight	Thickness			mm	in.	mm	in.
			mm	in.					
002-1-c	1	Molybdenum	0.0508	0.0020	(a)	0.0599	0.0022	0.0584	0.0023
	2	82.58Mo-17.42ZrO_2	.0508	.0020		.1448	.0057	.1346	.0053
	3	61.25Mo-38.75ZrO_2	.0508	.0020		------	------	------	------
	4	34.51Mo-65.49ZrO_2	.0508	.0020		------	------	------	------
	5	63.23HfO_2-36.77ZrO_2	.1016	.0040		.1371	.0054	.1016	.0040
		Total	0.3048	0.0120		0.3378	0.0133	0.2946	0.0116
002-2-c	1	Molybdenum	0.0508	0.0020	(b)	0.0762	0.0030	0.2464	0.0097
	2	82.58Mo-17.42ZrO_2	.0508	.0020		.1448	.0057	------	------
	3	61.25Mo-38.75ZrO_2	.0508	.0020		------	------	------	------
	4	31.51Mo-65.49ZrO_2	.0508	.0020		.0710	.0028	.0940	.0037
	5	63.25HfO_2-36.77ZrO_2	.1016	.0040		------	------	------	------
		Total	0.3048	0.0120		0.2920	0.0115	0.3404	0.0134
002-3-c	1	Molybdenum	0.0508	0.0020	(d)	0.1651	0.0065	0.2388	0.0094
	2	82.58Mo-17.42ZrO_2	.0508	.0020		------	------	------	------
	3	61.25Mo-38.75ZrO_2	.0508	.0020		------	------	------	------
	4	34.51Mo-65.49ZrO_2	.0508	.0020		------	------	------	------
	5	63.23HfO_2-36.77ZrO_2	.1016	.0040		.1295	.0051	------	------
		Total	0.3048	0.0120		0.2946	0.0116	0.2388	0.0094
006-1-c	1	95W-5 Nicoro 80	0.1016	0.0040	(a)	0.5436	0.0214	0.4140	0.0163
	2	85W-12ZrO_2-3Cu	.5080	.0200		------	------	------	------
		Total	0.6096	0.0240		0.5436	0.0214	0.4140	0.0163
006-2-c	1	95W-5 Nicoro 80	0.1016	0.0040	(b)	0.6147	0.0242	0.5613	0.0221
	2	85W-12ZrO_2-3Cu	.5080	.0200		------	------	------	------
		Total	0.6096	0.0240		0.6147	0.0242	0.5613	0.0221
008-3-c	1	Chromium	0.0508	0.0020	(a)	0.0254	0.0010	0.0508	0.0020
	2	56Ni-14Cr-30Cr_2O_3	.0508	.0020		.1245	.0049	.1829	.0072
	3	24Ni-6Cr-70Cr_2O_3	.0508	.0020		------	------	------	------
	4	8Ni-2Cr-90Cr_2O_3	.0508	.0020		------	------	------	------
	5	Chromia	.1016	.0040		.1320	.0052	------	------
		Total	0.3048	0.0120		0.2819	0.0111	0.2337	0.0092
008-2-c	1	Chromium	0.0508	0.0020	(b)	0.1498	0.0059	0.1219	0.0048
	2	56Ni-14Cr-30Cr_2O_3	.0508	.0020		.0686	.0027	.1245	.0049
	3	24Ni-6Cr-70Cr_2O_3	.0508	.0020		------	------	------	------
	4	8Ni-2Cr-90Cr_2O_3	.0508	.0020		------	------	------	------
	5	Chromia	.1016	.0040		.0737	.0029	------	------
		Total	0.3048	0.0120		0.2920	0.0115	0.2464	0.0097
020-3-c	1	Molybdenum	0.0508	0.0020	(a)	0.0584	0.0023	0.0686	0.0027
	2	82.58Mo-17.42ZrO_2	.0508	.0020		.1295	.0051	.1854	.0073
	3	61.25Mo-38.75ZrO_2	.0508	.0020		------	------	------	------
	4	34.51Mo-65.49ZrO_2	.0508	.0020		------	------	------	------
	5	63.23HfO_2-36.77ZrO_2	.1016	.0040		.1245	.0049	.0686	.0027
		Total	0.3048	0.0120		0.3124	0.0123	0.3226	0.0127
020-2-c	1	Molybdenum	0.0508	0.0020	(b)	0.0508	0.0020	0.0559	0.0022
	2	82.58Mo-17.42ZrO_2	.0508	.0020		.1092	.0043	.1397	.0055
	3	61.25Mo-38.75ZrO_2	.0508	.0020		.0533	.0021	------	------
	4	34.51Mo-65.49ZrO_2	.0508	.0020		------	------	------	------
	5	63.23HfO_2-36.77ZrO_2	.1016	.0040		.1295	.0051	.0914	.0036
		Total	0.3048	0.0120		0.3428	0.0135	0.2870	0.0113

[a] H_2 environment at 24.5×10^6 W/m^2 (15 Btu/(in.^{2})(sec)) in 2-minute cycles for a total time of 30 minutes duration.

[b] H_2O_2 environment at 24.5×10^6 W/m^2 (15 Btu/(in.^{2})(sec)) in 5-minute cycles for a total time of 30 minutes duration.

[d] 10-hour test.

TABLE II. - SUMMARY OF COATING SYSTEM MATERIAL AND EXPERIMENTAL PROCEDURES FOLLOWED IN COATING SYSTEM SAMPLE STUDY

(a) Summary of coating system material[a]

Material	Supplier	Supplied stock number	Typical chemical analysis[a]	Average particle size			
				mm	in.	mm	in.
				As supplied		As sprayed	
Metals							
Molybdenum (Mo)	(b)	63	99.0% Mo	0.0560	0.0022	0.0300	0.0012
Nichrome	(c)	-----	---------	.0620	.0024	.0440	.0017
Tungsten (W)	(d)	117-M	---------	.0590	.0028	.0300	.0012
Copper (Cu)	(b)	55	99.0% Cu	.0560	.0022	↓	↓
Chromium (Cr)	(c)	-----	99.8% Cr	.0590	.0023		
Nickel (Ni)	(d)	112-M	---------	.0590	.0023		
Nicoro 80	(e)	14844	81.5% Au; 16.5% Cu; 2.0% Ni	.0440	.0017		
Oxides							
Zirconia (CaO)	(b)	201-B	93% ZrO_2; 0.5% Al_2O_3; 4.0% CaO; 0.4% SiO_2 Bal.	0.0530	0.0021	0.0300	0.0012
Zirconia (Y_2O_3)	(f)	Special	88% ZrO_2; 12% Y_2O_3	.0590	.0023	↓	↓
Alumina	(d)	300-M	99.53% Al_2O_3; 0.04% SiO_2; 0.10% Fe_2O_3; 0.33% NaO	.0590	.0023		
Hafnia	(f)	1547	95% HfO_2; 5% Y_2O_3	.0740	.0029		
Chromia	(d)	309-M	99.0% Cr_2O_3; SiO_2; Fe_2O_3; NaO; CaO traces	.0500	.0019		
Mixtures							
83.2% Mo-16.8% ZrO_2	(f)	Special		0.0125	0.0005	0.0125	0.0005
62.5% Mo-37.5% ZrO_2	(f)	Special		.0125	.0005	.0125	.0005
35.5% Mo-64.5% ZrO_2	(f)	Special		.0125	.0005	.0125	.0005

[a]All samples grit-blasted with 60 mesh alumina particles to 3.175 rms μm (125 rms μin.) roughness.

[b]Metco, Inc., 1109 Prospect Ave., Westbury Long Island, New York, 11590.

[c]Atlantic Equipment Engineers, 181 Reid Ave., Bergenfield, New Jersey, 07621.

[d]Plasmadyne, 3839 South Main St., Santa Ana, California, 92702.

[e]Western Gold and Platinum Company, 525 Harbor Blvd., Belmont, California, 94002.

[f]Cerac, Inc., P.O. Box 597, Butler, Wisconsin, 53007.

TABLE II. - Concluded. SUMMARY OF COATING SYSTEM MATERIAL AND EXPERIMENTAL PROCEDURES FOLLOWED IN COATING SYSTEM SAMPLE STUDY

(b) Summary of experimental procedures followed

Phase	Step
Sample pretest examinations	1. Record photographs taken: a. Full view (color) b. Magnified (X3) of surface (monochrome) 2. Examine surface microscopically for detail. 3. Take coating scrapings from tube ends for post-test X-ray diffraction.
Sample cold-shock conditioning	1. Cool sample rapidly with liquid nitrogen (in tubes) from ambient temperature. 2. Allow sample to return to ambient temperature. 3. Reexamine surface microscopically for changes.
Sample hot testing	(HYDROGEN) 1. Endurance test for 30 minutes (noncontinuous) at 2 minutes per cycle for 15 cycles. Heat flux level of 24.5×10^6 W/m^2 (15 Btu/(in.^{2})(sec)). 2. Endurance test for 30 minutes (noncontinuous). Heat flux level of 19.6×10^6 W/m^2 (12 Btu/(in.^{2})(sec)). 3. 10-Hour duration test for 600 minutes (noncontinuous) at 6 minutes per cycle for 100 cycles. Heat flux level of 16.3×10^6 W/m^2 (10 Btu/(in.^{2})(sec)).
	(HYDROGEN-OXYGEN) 1. Endurance test for 30 minutes (noncontinuous) at 5 minutes per cycle for 6 cycles. Heat flux level of 24.5×10^6 W/m^2 (15 Btu/(in.^{2})(sec)).
Sample post-test examinations	1. Record photographs taken: a. Full view (color) b. Magnified (X3) of surface (monochrome) 2. Reexamine surface microscopically for changes. 3. Take coating scrapings from tested area for X-ray diffraction comparisons. 4. Make sections at tube ends and heat area and photomicrograph (used for coating thickness measurements and structural change studies).

TABLE III. - EFFECT OF PLASMA EXPOSURE ON VARIOUS COATING SYSTEMS

(a) Simple coating systems

Coating system sample	Test cycle	Pretesting		Post-testing			
		Visual appearance	Surface X-ray diffraction indications	Visual appearance	Surface X-ray diffraction indications	Thickness loss	
						mm	in.
017-1-c	(a)	White to light gray; smooth surface	Cubic γ-Al_2O_3; hexagonal α-Al_2O_3	Light gray on heated zone; remaining portion to sample was dark brown to tan; top surface suffered severe surface erosion.	Body-centered cubic molybdenum (strong); hexagonal α-Al_2O_3 (good crystal)	0.2363	0.0093
017-2-c	(b)	White to light gray; smooth surface	Cubic γ-Al_2O_3; hexagonal α-Al_2O_3		Cubic η-Al_2O_3 spinel; rhombic β-$Al_2O_3 \cdot H_2O$ (trihydrate); hexagonal α-Al_2O_3	0.3987	0.0157
018-3-c	(a)	Light buff to creamy yellow	Face-centered cubic ZrO_2	Light golden color with small cracks.	Face-centered cubic ZrO_2; face-centered cubic ZrN; body-centered cubic molybdenum	0.2133	0.0084
018-2-c	(b)	Light buff to creamy yellow	Face-centered cubic ZrO_2		Face-centered cubic ZrO_2	0.3276	0.0129
019-3-c	(a)	Light buff to creamy yellow	Face-centered cubic ZrO_2		Face-centered cubic ZrO_2	0.2108	0.0083
019-2-c	(b)	Light buff to creamy yellow	Face-centered cubic ZrO_2		Face-centered cubic ZrO_2	0.0406	0.0016
021-1-c	(a)	White to light gray with minute black flecks upon surface	Face-centered cubic γ-Al_2O_3; body-centered cubic molybdenum; hexagonal α-Al_2O_3 (strong)	Dark to light gray in center zone with remaining portion of sample buff to white.	Hexagonal α-Al_2O_3; body-centered cubic molybdenum	0.1752	0.0069
021-2-c	(b)	White to light gray with minute black flecks upon surface	Face-centered cubic γ-Al_2O_3; body-centered cubic molybdenum; hexagonal α-Al_2O_3 (strong)		Face-centered cubic γ-Al_2O_3; hexagonal α-Al_2O_3 (very strong); body-centered cubic molybdenum (weak)	0.1498	0.0059
022-1-c	(a)	Light buff to creamy yellow	Body-centered cubic molybdenum; face-centered cubic ZrO_2	Light golden color in heated zone with mud flat cracks; fringe area of heated zone was silvery gray to light tan.	Face-centered cubic ZrN; face-centered cubic ZrO_2	0.0127	0.0005
022-2-c	(b)	Light buff to creamy yellow	Body-centered cubic molybdenum; face-centered cubic ZrO_2		Face-centered cubic ZrO_2; body-centered cubic molybdenum; monoclinic ZrO_2	0.0228	0.0009
023-1-c	(a)	White smooth surface	Face-centered cubic ZrO_2	Heated zone had golden to dark brown color; cellular cracks associated with minute chuck holes and coating was flacked away.	Face-centered cubic ZrN; face-centered cubic ZrO_2	0.0788	0.0031
023-2-c	(b)	White smooth surface	Face-centered cubic ZrO_2		Body-centered cubic molybdenum (weak); face-centered cubic ZrO_2	0.1549	0.0061

[a] H_2 environment at 24.5×10^6 W/m^2 (15 Btu/(in.^{2})(sec)) in 2-minute cycles for a total time of 30 minutes duration.
[b] H_2-O_2 environment at 24.5×10^6 W/m^2 (15 Btu/(in.^{2})(sec)) in 5-minute cycles for a total time of 30 minutes duration.

TABLE III. - Continued. EFFECT OF PLASMA EXPOSURE ON VARIOUS COATING SYSTEMS

(b) Layered coating systems

Coating system sample	Test cycle	Pretesting		Post-testing			
		Visual appearance	Surface X-ray diffraction indications	Visual appearance	Surface X-ray diffraction indications	Thickness loss	
						mm	in.
004-3-c	(a)	White to light gray	Cubic γ-Al_2O_3; hexagonal α-Al_2O_3		Hexagonal α-Al_2O_3	0.0331	0.0013
004-2-c	(b)	White to light gray	Cubic γ-Al_2O_3; hexagonal α-Al_2O_3		Face-centered cubic molybdenum; face-centered cubic nickel; nickel silicide	0.1321	0.0052
005-1-c	(a)	Light buff smooth surface	Face-centered cubic ZrO_2	Heated zone displayed bright golden metallic to light yellowish brown; small mud flat cracks in heated zone.	Face-centered cubic ZrN; face-centered cubic ZrO_2	0.0280	0.0011
005-2-c	(b)	Light buff smooth surface	Face-centered cubic ZrO_2		Body-centered cubic molybdenum; face-centered cubic ZrO_2	0.0026	0.0001

[a] H_2 environment at 24.5×10^6 W/m^2 (15 Btu/(in.^{2})(sec)) in 2-minute cycles for a total time of 30 minutes duration.
[b] H_2-O_2 environment at 24.5×10^6 W/m^2 (15 Btu/(in.^{2})(sec)) in 5-minute cycles for a total time of 30 minutes duration.

TABLE III. - Continued. EFFECT OF PLASMA EXPOSURE ON VARIOUS COATING SYSTEMS

(c) Simple-graded coating systems

Coating system sample	Test cycle	Pretesting		Post-testing			
		Visual appearance	Surface X-ray diffraction indications	Visual appearance	Surface X-ray diffraction indications	Thickness loss	
						mm	in.
003-1-c	(a)	White to light gray surface	Cubic γ-Al_2O_3; hexagonal α-Al_2O_3	Heated zone displayed dark gray color with small blotches of dark spots; remaining portion of sample was white to gray.	Cubic γ-Al_2O_3; hexagonal α-Al_2O_3	0.0584	0.0023
003-2-c	(b)	White to light gray surface	Cubic γ-Al_2O_3; hexagonal α-Al_2O_3		Body-centered cubic molybdenum; nickel silicide; face-centered cubic nickel	0.2057	0.0081
007-1-c	(a)	Light buff color	Face-centered cubic ZrO_2	Bright golden spot in center of heated area; remaining portion of sample was black; small mud flat cracks with slight lifting up of coating.	Face-centered cubic ZrN; face-centered cubic ZrO_2	0.0229	0.0009
007-2-c	(b)	Light buff color	Face-centered cubic ZrO_2		Cubic α-Al_2O_3; face-centered cubic ZrO_2	0.0635	0.0025
001-1-c	(a)	Light buff to creamy yellow	Face-centered cubic ZrO_2	Heated zone displayed a bright golden color with small white blotches on its fringe area; mud flat and hairline cracks with metal globules emerging from crevices.	Face-centered cubic ZrN; face-centered cubic ZrO_2	0.0661	0.0026
001-2-c	(b)	Light buff to creamy yellow	Face-centered cubic ZrO_2	Heated zone displayed dark bluish-gray color; gray glazed surface area; small isolated beads of metallic Nichrome metal surrounding mud flat cracks giving a reticulated-like surface appearance.	Face-centered cubic ZrO_2; body-centered cubic molybdenum	0.0152	0.0006
001-3-c	(c)	Light buff to creamy yellow	Face-centered cubic ZrO_2		Face-centered cubic ZrO_2; face-centered cubic nickel; trace of hafnium	0.0355	0.0014

[a] H_2 environment at 24.5×10^6 W/m^2 (15 Btu/(in.^{2})(sec)) in 2-minute cycles for a total time of 30 minutes duration.
[b] H_2-O_2 environment at 24.5×10^6 W/m^2 (15 Btu/(in.^{2})(sec)) in 5-minute cycles for a total time of 30 minutes duration.
[c] Helium environmental purge.

TABLE III. - Concluded. EFFECT OF PLASMA EXPOSURE ON VARIOUS COATING SYSTEMS

(d) Compound-graded coating systems

Coating system sample	Test cycle	Pretesting		Post-testing			
		Visual appearance	Surface X-ray diffraction indications	Visual appearance	Surface X-ray diffraction indications	Thickness loss	
						mm	in.
002-1-c	(a)	Tan to light buff color with black metallic flecks on surface top.	Face-centered cubic ZrO_2; body-centered cubic molybdenum	Heated zone experienced subsurface melting with metallic beads at outer fringe area of center zone; dark golden color with mud flat cracks appearing in geometrical pattern.	Face-centered cubic ZrN; face-centered cubic ZrO_2	0.0432	0.0017
002-2-c	(b)	Tan to light buff color with black metallic flecks on top surface.	Face-centered cubic ZrO_2; body-centered cubic molybdenum	Crack in heated zone along with swelling of coating top layer.	Face-centered cubic ZrO_2; body-centered cubic molybdenum	0.0484	0.0019
002-3-c	(d)	Tan to light buff color with black metallic flecks on top surface.	Face-centered cubic ZrO_2; body-centered cubic molybdenum	Light buff to light golden color at heated zone; cellular-shaped mud flat cracking having glazed appearance; remaining portion of sample was dark gray to black	Face-centered cubic ZrN (strong); face-centered cubic ZrO_2 (strong); body-centered cubic molybdenum (strong)	0.0558	0.0022
006-1-c	(a)		Body-centered cubic tungsten (strong); face-centered cubic copper; face-centered cubic ZrO_2; face-centered cubic gold		Body-centered cubic tungsten (strong); face-centered cubic copper (weak); face-centered cubic ZrO_2 (weak); tungsgen oxide	0.1296	0.0051
006-2-c	(b)		Body-centered cubic tungsten (strong); face-centered cubic copper; face-centered cubic ZrO_2; face-centered cubic gold		Body-centered cubic tungsten (strong); face-centered cubic ZrO_2 (weak); tungsten oxide	0.0533	0.0021
008-3-c	(a)	Dark silvery gray to dark brown with metallic globules throughout surface.	Body-centered cubic chromium; rhombic Cr_2O_3; face-centered cubic nickel		Rhombic Cr_2O_3; face-centered cubic nickel; CrNi	0.0482	0.0019
008-2-c	(b)	Dark silvery gray to dark brown with metallic globules throughout surface.	Body-centered cubic chromium; rhombic Cr_2O_3; face-centered cubic nickel		Rhombic Cr_2O_3; face-centered cubic nickel	0.0456	0.0018
020-3-c	(a)		Body-centered cubic molybdenum; face-centered cubic ZrO_2		Face-centered cubic ZrO_2; face-centered cubic ZrN; zirconium (strong); hafnium (weak); yttria (trace); molybdenum (trace)	0.0102	0.0004
020-2-c	(b)		Body-centered cubic molybdenum; face-centered cubic ZrO_2		Monoclinic ZrO_2; face-centered cubic ZrO_2; body-centered cubic molybdenum	0.0558	0.0022

[a] H_2 environment at 24.5×10^6 W/m^2 (15 Btu/(in.^{2})(sec)) in 2-minute cycles for a total time of 30 minutes duration.
[b] H_2-O_2 environment at 24.5×10^6 W/m^2 (15 Btu/(in.^{2})(sec)) in 5-minute cycles for a total time of 30 minutes duration.
[d] 10-hour test.

TABLE IV. - THERMAL CONDUCTIVITIES OF VARIOUS COATING SYSTEMS

(a) Simple coating systems

Sample	Coating mean temperature		Thermal conductivity	
	K	^{o}R	W/(m)(K)	Btu/(in.)(sec)(^{o}R)
017-1-c	722	1300	0.6939	0.0929×10^{-4}
	880	1585	1.076	.1439
	1004	1807	1.3920	.1863
	1105	1990	1.6760	.2243
	1192	2145	1.9470	.2605
	1229	2212	2.3410	.3132
	1273	2292	2.6970	.3609
	1340	2415	2.9790	.3986
018-1-c	794	1430	1.6500	0.2208×10^{-4}
	873	1572	2.2900	.3064
	978	1760	2.6640	.3564
	1122	2020	2.7380	.3664
	1308	2355	2.6340	.3524
019-1-c	825	1485	0.9918	0.1327×10^{-4}
	922	1662	1.3270	.1776
	1025	1845	1.5730	.2104
	1222	2200	1.5160	.2030
	1353	2435	1.6080	.2152
	1389	2507	1.8660	.2497
021-1-c	728	1310	0.4533	0.0606×10^{-4}
	790	1423	.8774	.1174
	874	1573	1.2050	.1612
	922	1665	1.5550	.2102
	969	1745	1.9380	.2594
	1030	1855	2.2150	.2964
	1059	1907	2.6260	.3511
022-1-c	711	1280	0.3759	0.0503×10^{-4}
	866	1565	.5785	.0774
	939	1692	.8259	.1105
	986	1775	1.0920	.1461
	1039	1870	1.3280	.1777
	1132	2037	1.4410	.1928
	1329	2392	1.3090	.1751
	1455	2620	1.5770	.2110
	1409	2537	1.9480	.2606
	1439	2590	2.1530	.2881
023-1-c	766	1380	0.8131	0.1088×10^{-4}
	893	1607	1.0030	.1342
	964	1735	1.2560	.1680
	1039	1870	1.4580	.1951
	1103	1985	1.6680	.2232
	1184	2132	1.7930	.2399
	1322	2382	1.7630	.2359
	1436	2585	1.7760	.2376
	1603	2885	1.6780	.2245
	1691	3045	1.7370	.2324
	1717	3092	1.9170	.2565

TABLE IV. - Continued. THERMAL CONDUCTIVITIES

OF VARIOUS COATING SYSTEMS

(b) Layered coating systems

Sample	Coating mean temperature		Thermal conductivity	
	K	^{o}R	W/(m)(K)	Btu/(in.)(sec)(^{o}R)
004-3-c	2081	3747	2.5490	0.3411×10^{-4}
005-1-c	722	1320	0.5643	0.0755×10^{-4}
	816	1475	1.0310	.1380
	918	1652	1.3780	.1844
	972	1755	1.7800	.2382
	1039	1870	2.1170	.2832
	1133	2040	2.2910	.3065
	1256	2262	2.3150	.3097
	1338	2400	2.5230	.3376
	1461	2630	2.4960	.3339
	1572	2830	2.5210	.3373

TABLE IV. - Continued. THERMAL CONDUCTIVITIES

OF VARIOUS COATING SYSTEMS

(c) Simple-graded coating systems

Sample	Coating mean temperature		Thermal conductivity	
	K	^{o}R	W/(m)(K)	Btu/(in.)(sec)(^{o}R)
001-1-c	728	1310	0.7273	0.0973×10^{-4}
	983	1770	.9417	.1260
	1326	2387	.9372	.1254
	1443	2597	1.1030	.1476
	1550	2790	1.3430	.1798
	1705	3070	1.4470	.1936
	1767	3182	1.6500	.2208
003-1-c	797	1435	1.367	0.1830×10^{-4}
	982	1767	1.524	.2039
	1132	2040	1.686	.2256
	1250	2250	1.880	.2516
	1366	2460	2.037	.2726
	1438	2592	2.269	.3037
	1483	2670	2.605	.3485
	1499	2750	2.889	.3866
	1672	3010	2.839	.3798
	1801	3242	2.838	.3797
	2017	3632	2.654	.3551
007-1-c	722	1300	0.8214	0.1099×10^{-4}
	833	1540	1.3420	.1796
	1028	1850	1.5800	.2114
	1166	2100	1.8050	.2415
	1228	2210	2.1850	.2923
	1272	2290	2.6010	.3480
	1400	2532	2.6620	.3562
	1522	2740	2.8040	.3752
	1558	2805	3.1410	.4202
	1658	2985	3.2410	.4337

TABLE IV. - Concluded. THERMAL CONDUCTIVITIES

OF VARIOUS COATING SYSTEMS

(d) Compound-graded coating systems

Sample	Coating mean temperature		Thermal conductivity	
	K	^{o}R	W/(m)(K)	Btu/(in.)(sec)(^{o}R)
002-1-c	716	1290	0.7506	0.1004×10^{-4}
	800	1445	1.3670	.1829
	979	1762	1.5520	.2077
	1130	2035	1.7160	.2296
	1247	2245	1.9130	.2560
	1375	2475	2.0430	.2734
	1543	2777	2.0490	.2742
	1636	2945	2.2360	.2992
006-3-c	2008	3615	4.625	0.6188×10^{-4}
	2033	3665	4.524	.6053
008-1-c	742	1335	1.4320	0.1917×10^{-4}
	793	1427	2.1230	.2840
	841	1515	2.7750	.3713
020-1-c	719	1295	0.6831	0.0914×10^{-4}
	777	1400	1.3370	.1789
	824	1483	2.0120	.2692
	875	1575	2.6150	.3499
	919	1655	3.2230	.4312
	978	1760	3.6840	.4929
	1076	1937	3.7310	.4992
	1130	2035	4.1580	.5564
	1250	2255	3.9570	.5294
	1311	2360	4.2110	.5634
	1439	2590	4.0020	.5355
	1439	2590	4.3990	.5887

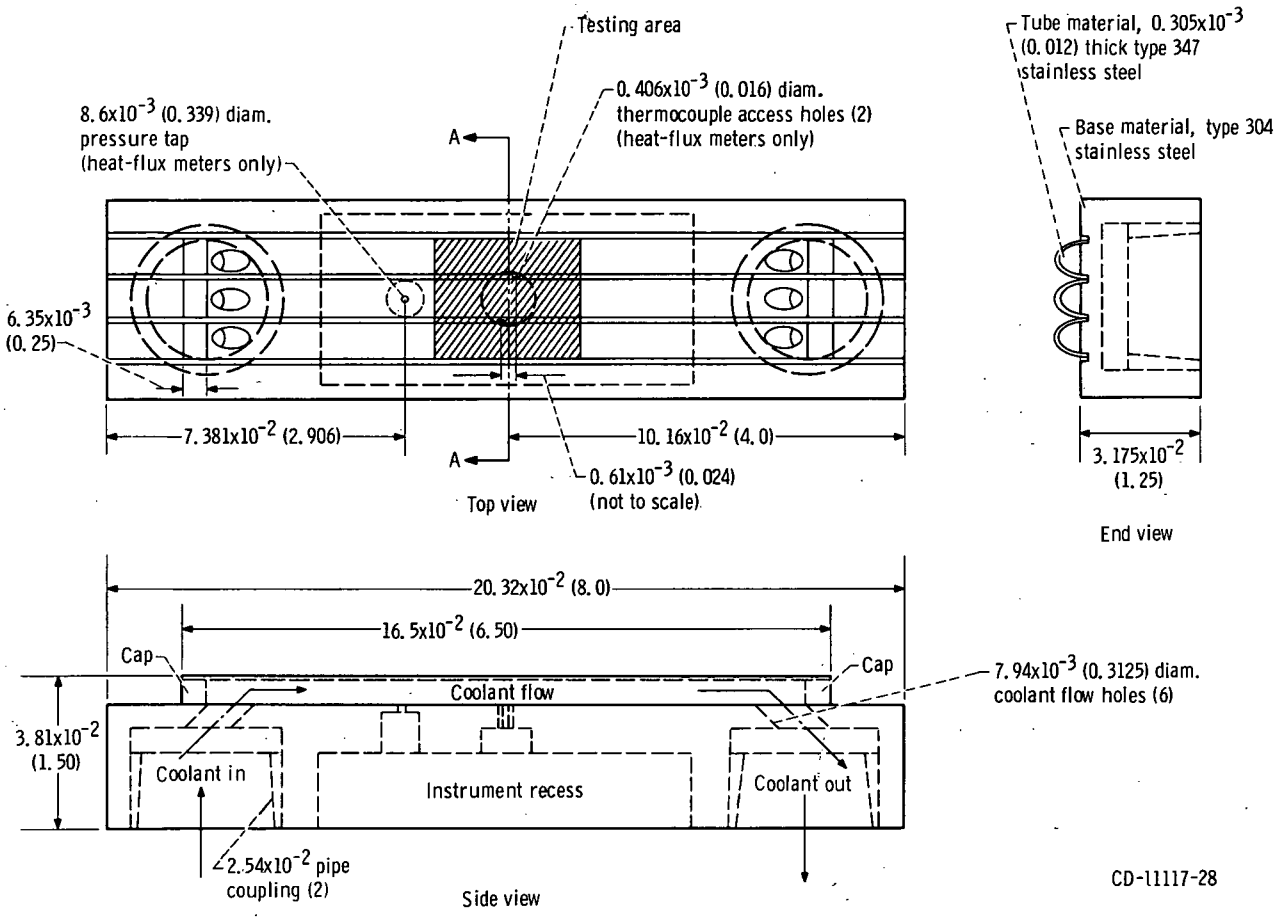

(a) General construction details.

Figure 1. - Coating system sample piece and heat-flux-meter configuration. (Dimensions are in meters (in.).)

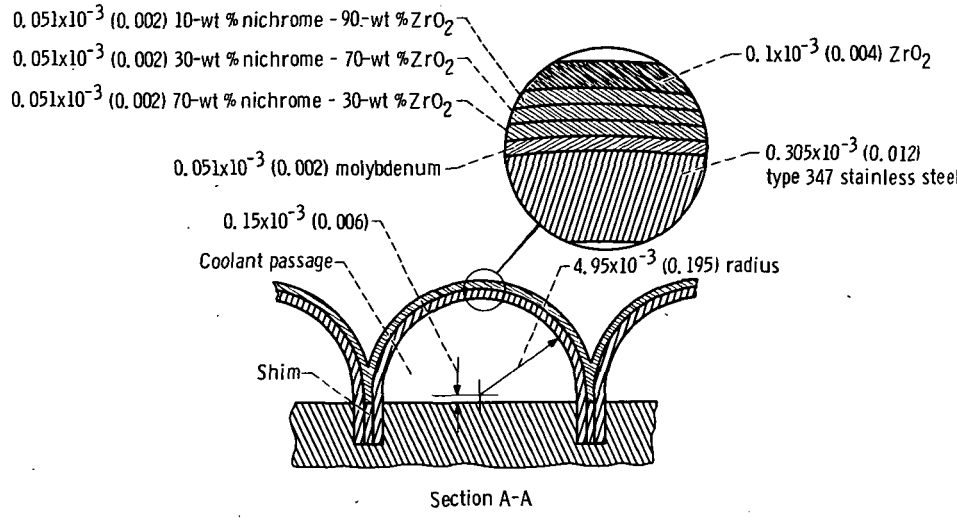

(b) Section view of sample piece with coating system (type 1) applied.

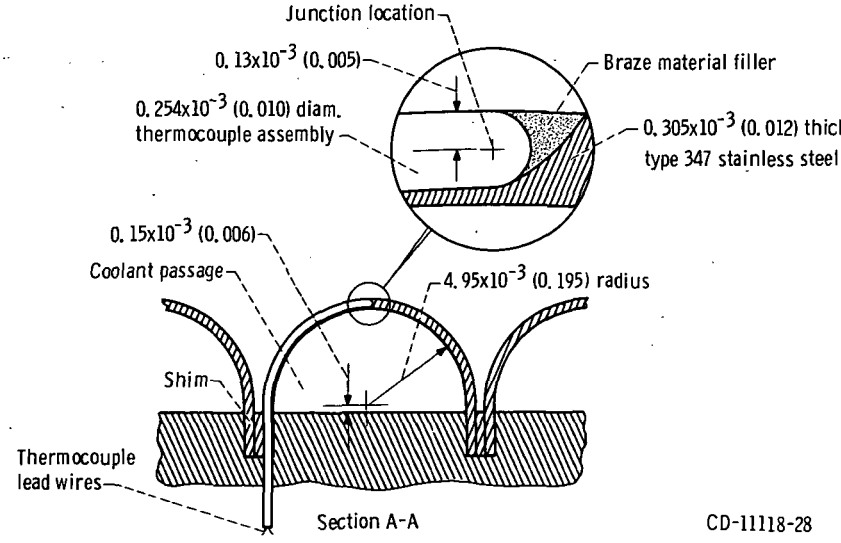

(c) Section view of heat-flux-meter version of sample piece.

Figure 1. - Concluded.

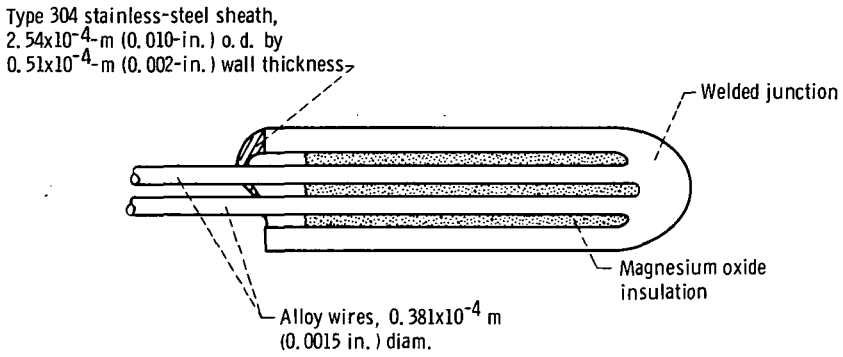

Figure 2. - Details of heat-flux-meter Chromel-Alumel thermocouple assembly.

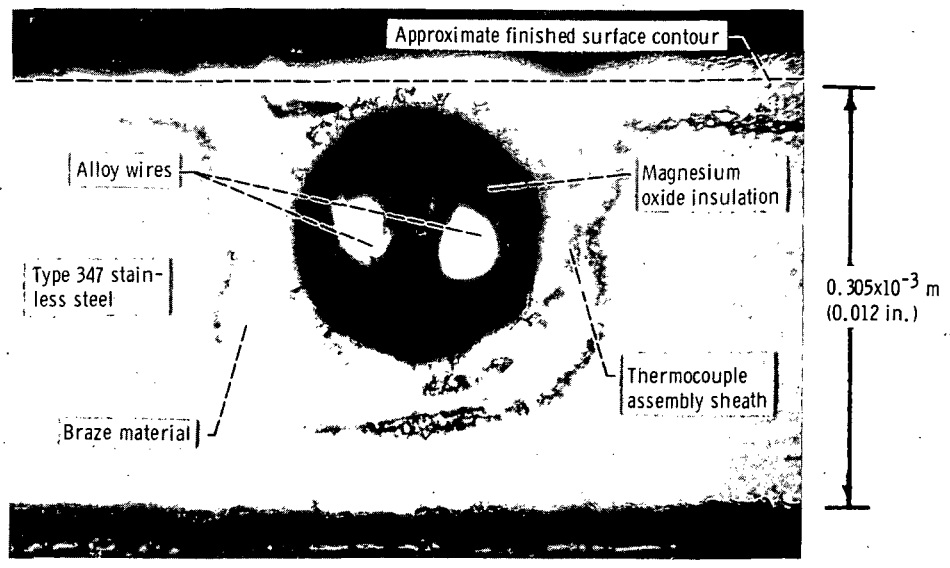

Figure 3. - Photomicrograph (originally X175 of section of 0.254×10^{-3}-meter (0.010-in.) diameter thermocouple assembly installed in 0.305×10^{-3}-meter (0.012-in.) thick type 347 stainless-steel wall. Section was made immediately behind thermocouple junction.

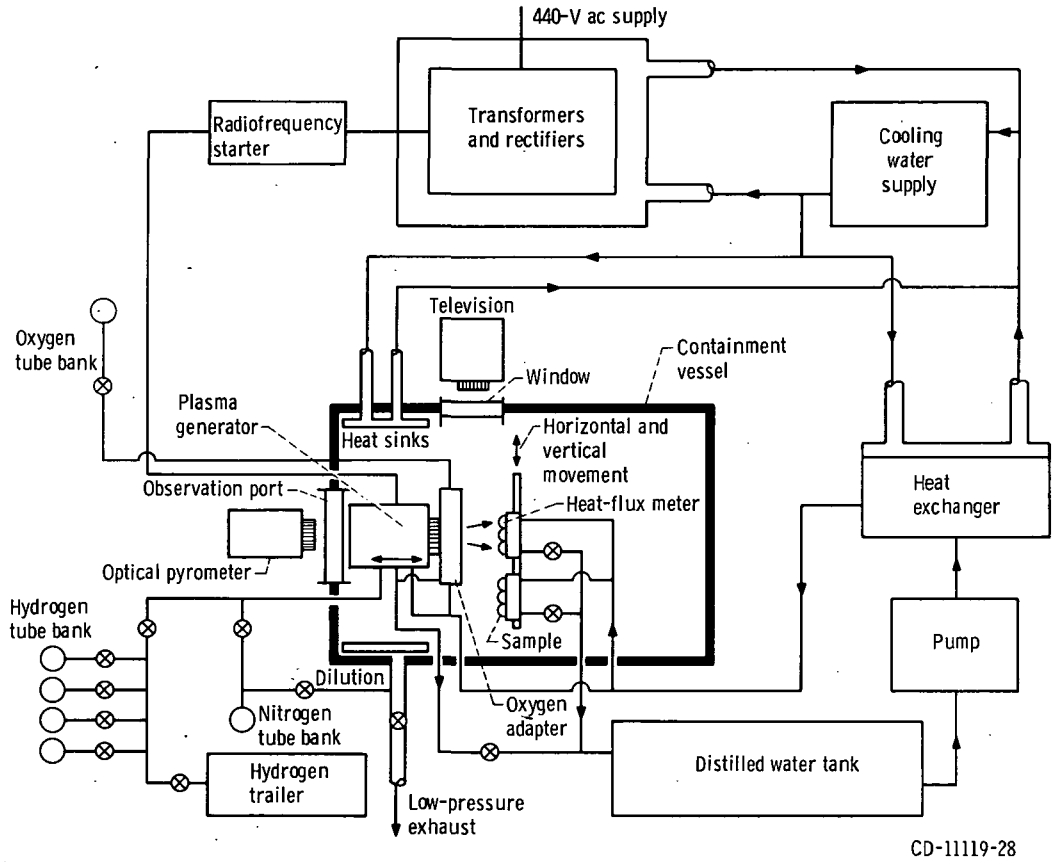

Figure 4. - Schematic of plasma generator test facility.

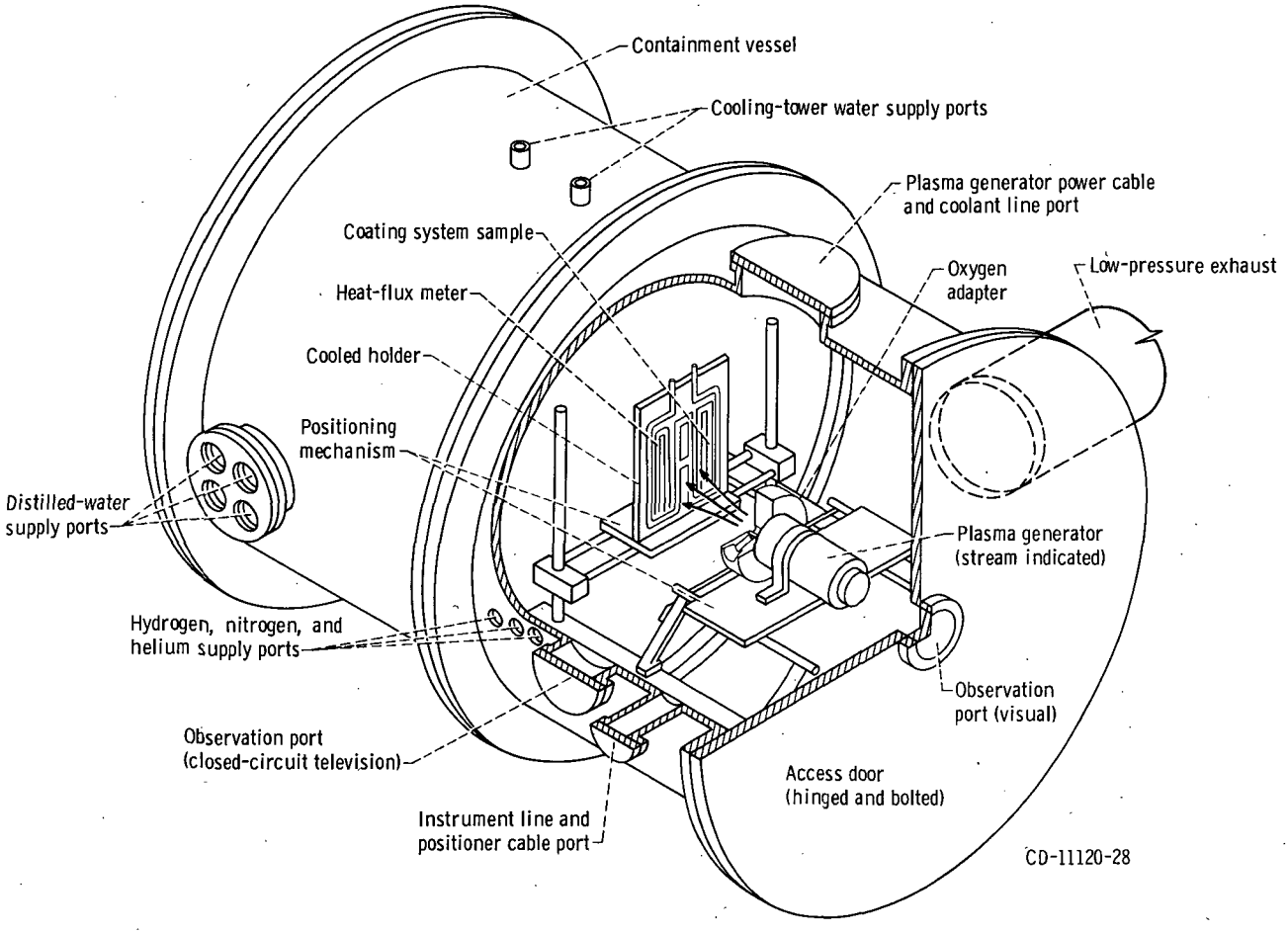

Figure 5. - Cutaway view of containment vessel, showing orientation of plasma generator, sample piece, and heat-flux meter. Tubes, cables, and hoses have been omitted here for clarity.

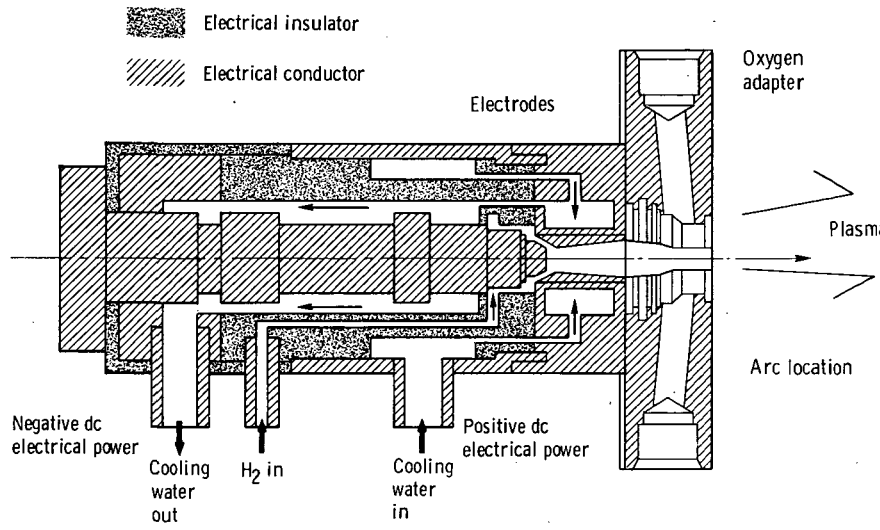

Figure 6. - Schematic of plasma generator used for heating coating system samples in this study. No scale intended.

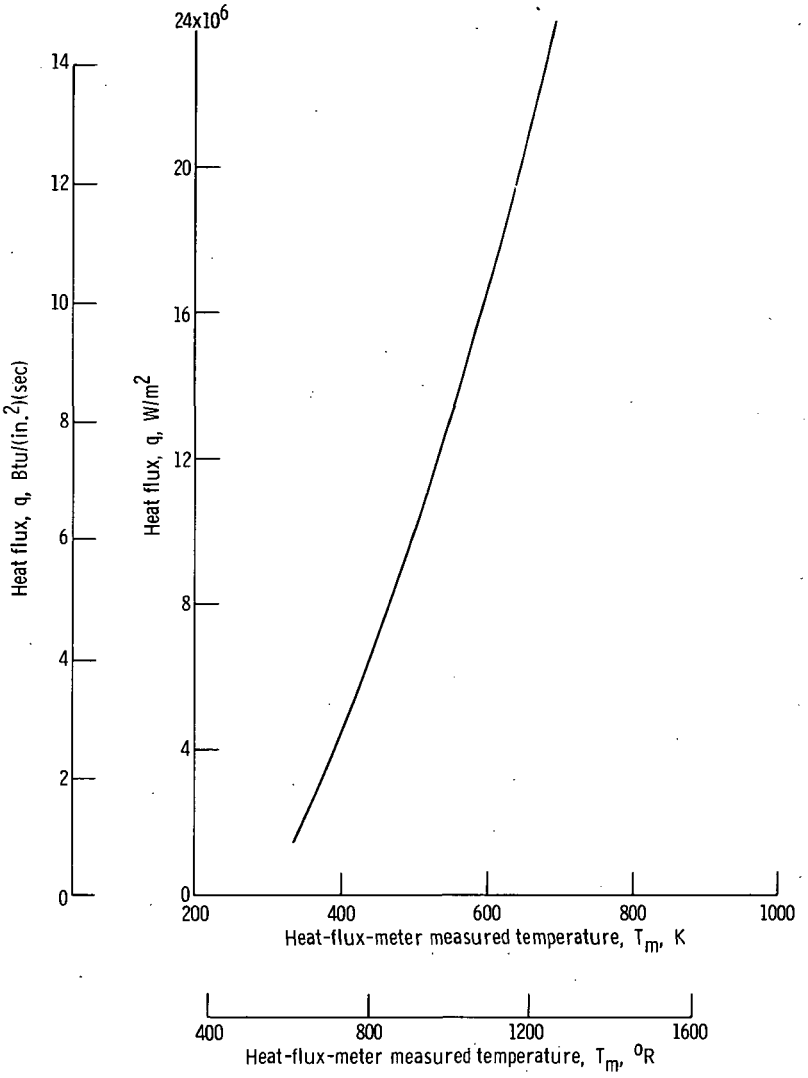

Figure 7. - Heat flux to heat-flux meter as function of measured temperature. Velocity of water, 26.274 meters per second (1034 in./sec); temperature of water, 305.25 K (550° R).

Layer	Coating system specifications for coated heat-flux meter		
	Material	Thickness	
		mm	in.
1	Molybdenum	0.089	0.0035
2	82.58-wt % Mo - 17.42-wt % ZrO_2	.064	.0025
3	61.25-wt % Mo - 38.75-wt % ZrO_2	.089	.0035
4	34.51-wt % Mo - 65.49-wt % ZrO_2	.064	.0025
5	63.23-wt % HfO_2 - 36.77-wt % ZrO_2	.076	.0030
	Total	0.382	0.0150

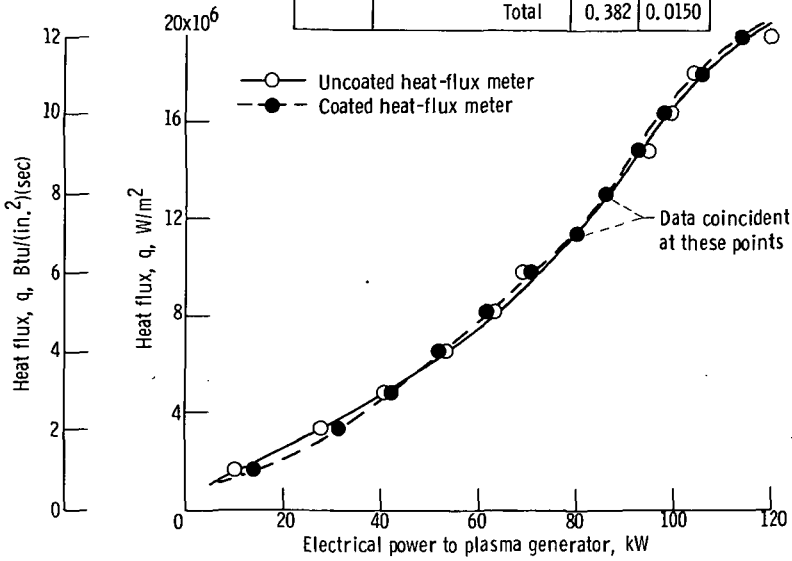

Figure 8. - Comparison of plasma generator electrical power levels for range of heat-flux levels for uncoated heat-flux meter and heat-flux meter protected by coating system representative of those investigated in this study. Hydrogen gas flow rate for both meters, 0.273×10^{-3} kilogram per second (0.0006 lbm/sec); spacing for both meters, 8.89×10^{-2} meter (3.5 in.).

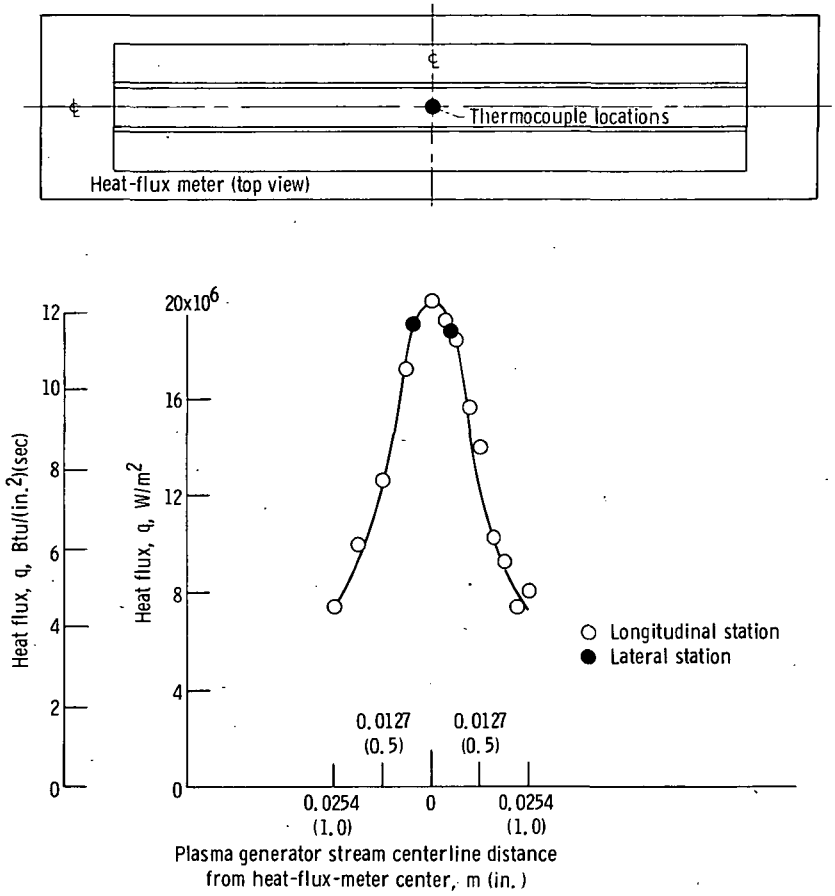

Figure 9. - Heat-flux profile near central position of heat-flux-meter center tube for nominal maximum heat flux of 19.6x10^6 W/m^2 (12 Btu/(in.^{2})(sec)). Hydrogen gas flow rate, 0.273x10^{-3} kilogram per second (0.0006 lbm/sec); spacing, 8.89x10^{-2} meter (3.5 in.).

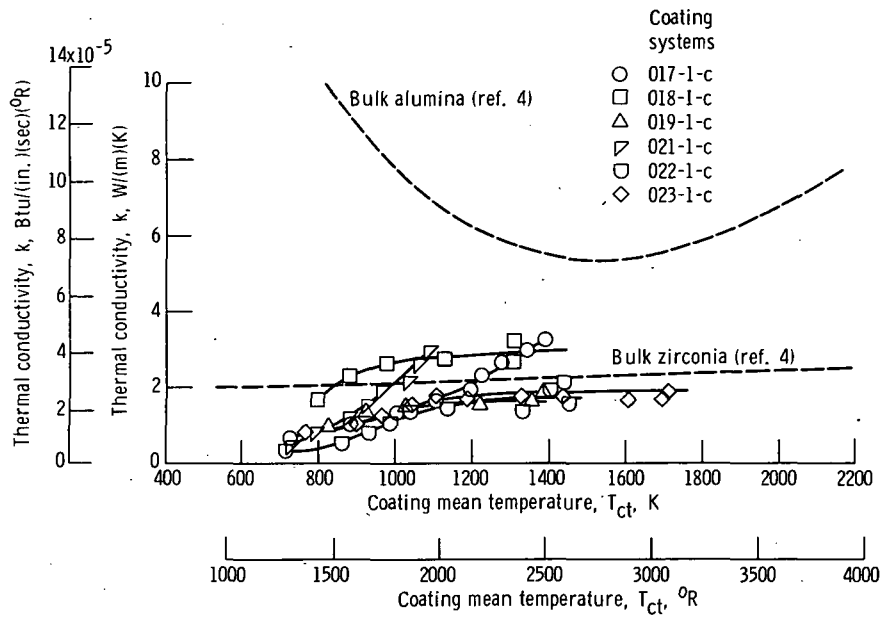

Figure 10. - Effective thermal conductivity of six simple coating systems as function of coating mean temperature.

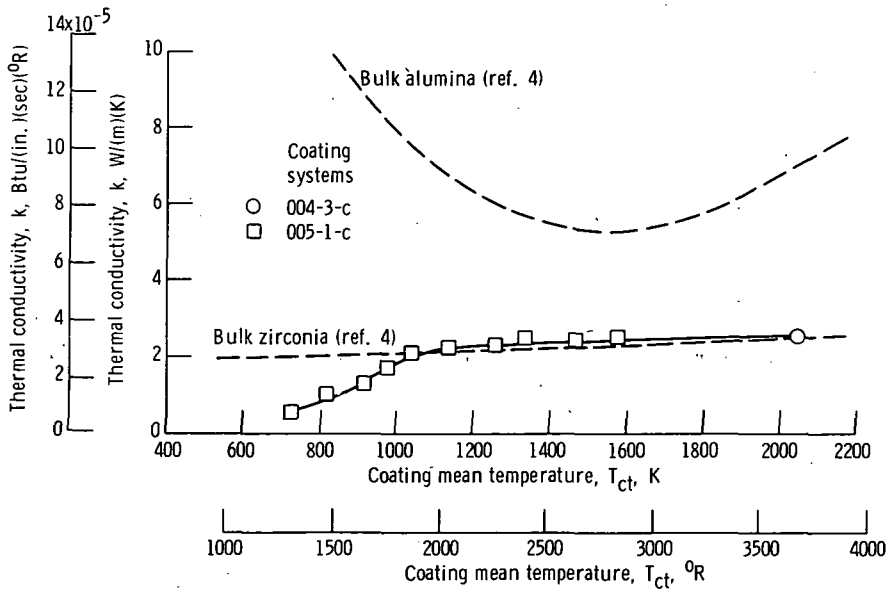

Figure 11. - Effective thermal conductivity of two-layered coating systems as function of coating mean temperature.

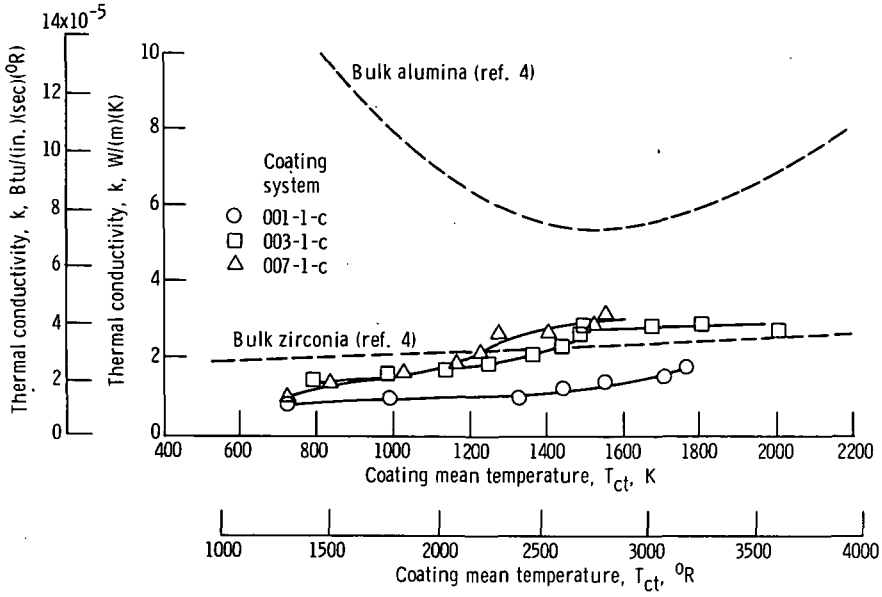

Figure 12. - Effective thermal conductivity of three simple-graded coating systems as function of coating mean temperature.

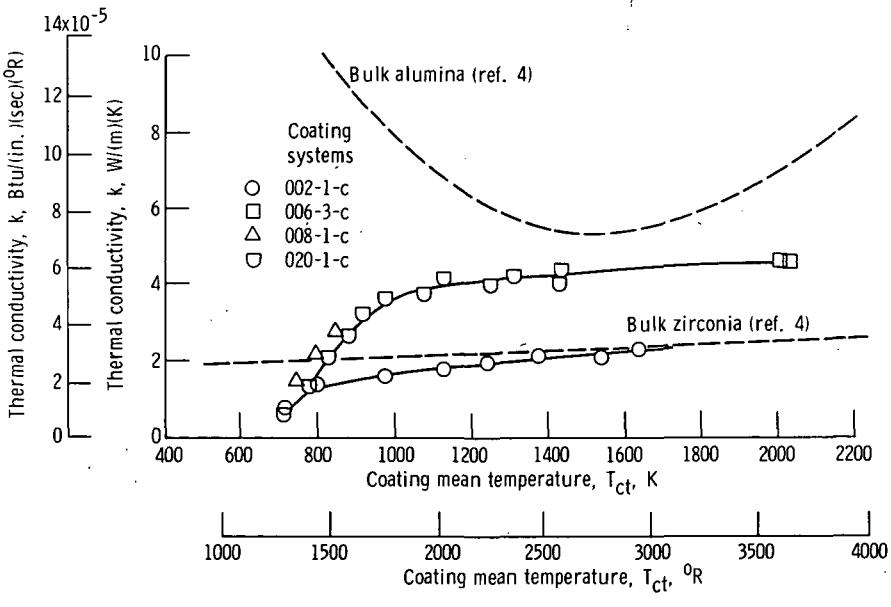

Figure 13. - Effective thermal conductivity of four compound-graded coating systems as function of coating mean temperature.

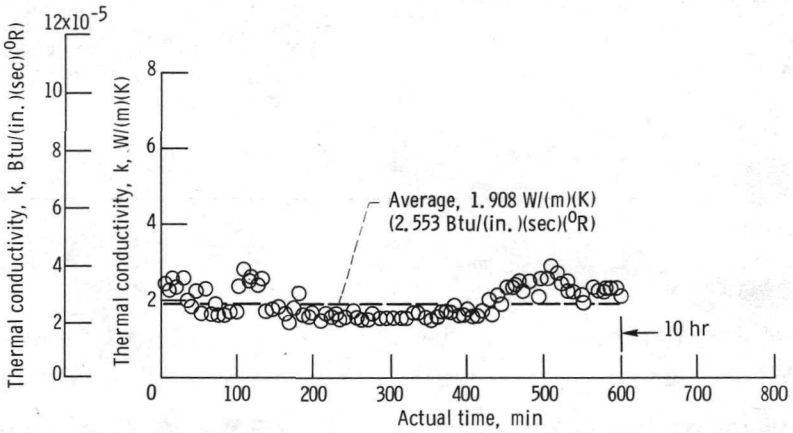

Figure 14. - Effective thermal conductivity of coating sample 002-3-c as function of time. Coating mean temperature, 1726 K (3107^{0} R); surface temperature, 2744 K (4940^{0} R).

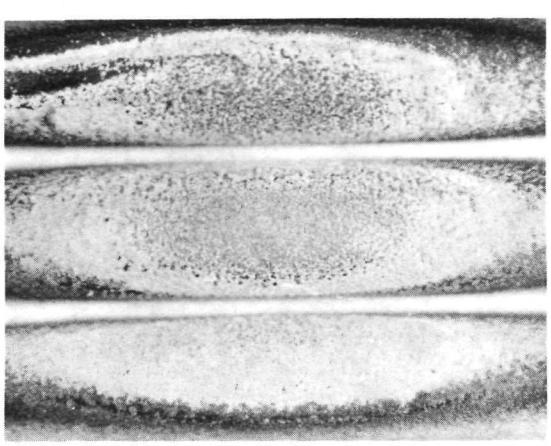

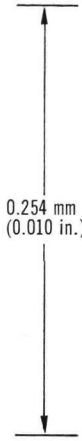

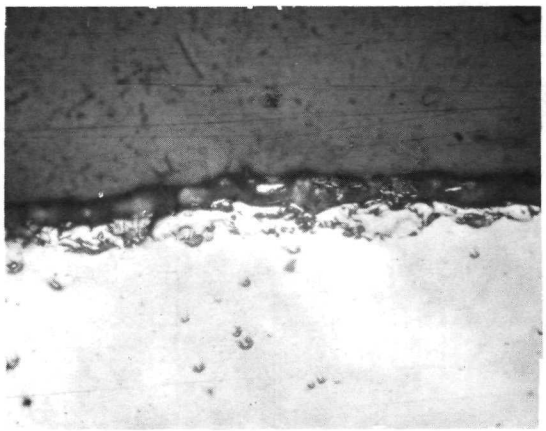

(a-1) Face view. Original photograph, X3.

(a-2) Section view. Original photomicrograph, X350.

(a) Views of coating system 021-1-c after testing in hydrogen plasma for 30 minutes at 24.5×10^6 W/m^2 (15 Btu/(in.^{2})(sec)).

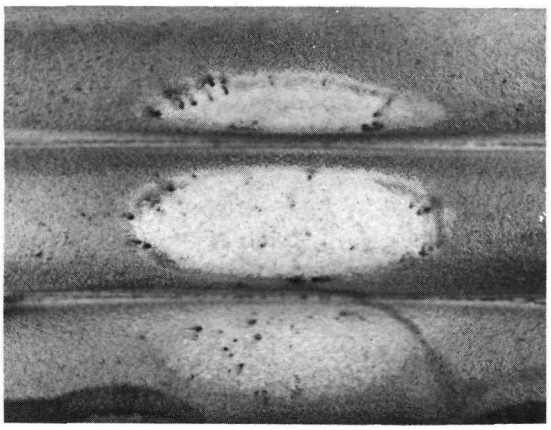

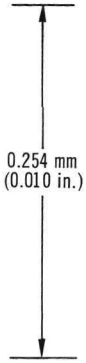

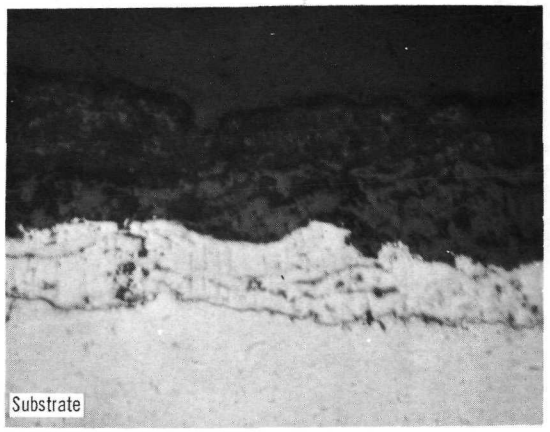

(b-1) Face view. Original photograph, X3.

(b-2) Section view. Original photomicrograph, X350.

(b) Views of coating system 021-2-c after testing in oxygen mixed with hydrogen plasma for 30 minutes at 24.5×10^6 W/m^2 (15 Btu/(in.^{2})(sec)).

Figure 15. - Structure effects on simple coating system 021 (Mo sublayer - Al_2O_3 outer layer) of plasma testing.

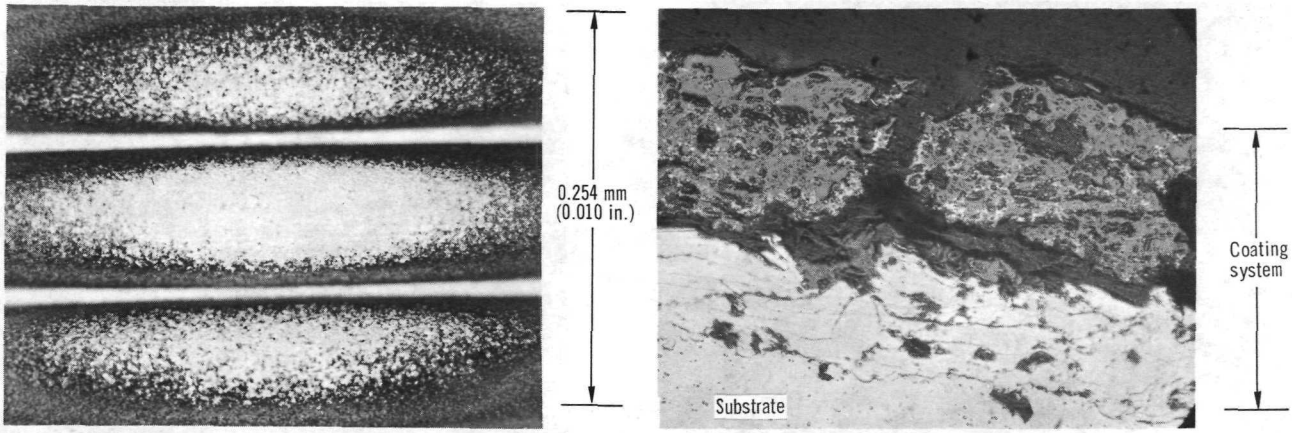

(a-1) Face view. Original photograph, X3.

(a-2) Section view. Original photomicrograph, X350.

(a) Views of coating system 022-1-c after testing in hydrogen plasma for 30 minutes at 24.5×10^6 W/m^2 (15 Btu/(in.^{2})(sec)).

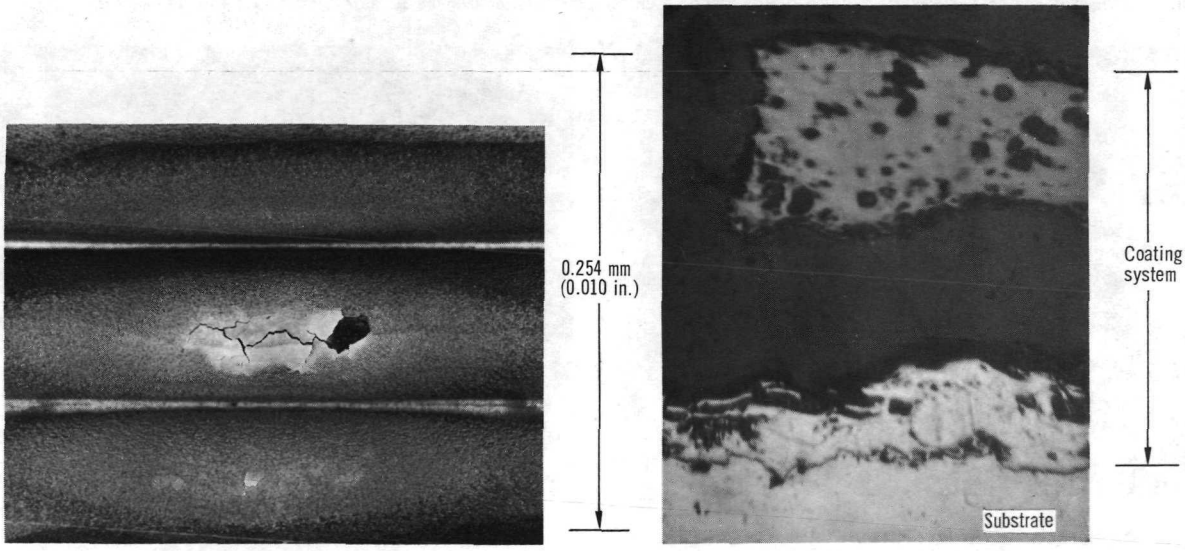

(b-1) Face view. Original photograph, X3.

(b-2) Section view. Original photomicrograph, X350.

(b) Views of coating system 022-1-c after testing in oxygen mixed with hydrogen plasma for 30 minutes at 24.5×10^6 W/m^2 (15 Btu/(in.^{2})(sec)).

Figure 16. - Structure effects on simple coating system 022 (Mo sublayer - ZrO_2 outer layer) of plasma testing.

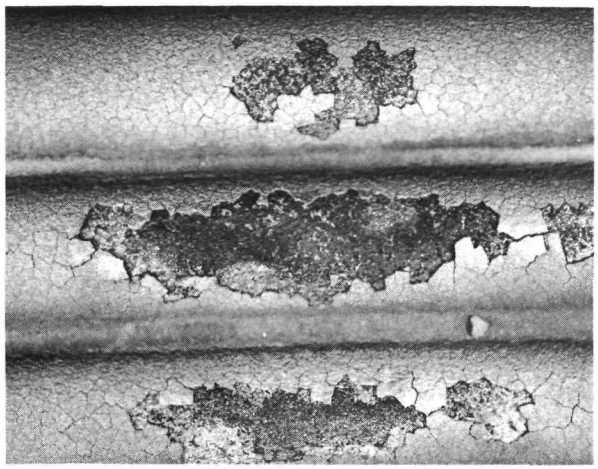

(a-1) Coating system sample 017-1-c (Mo sublayer - Al_2O_3 outer layer).

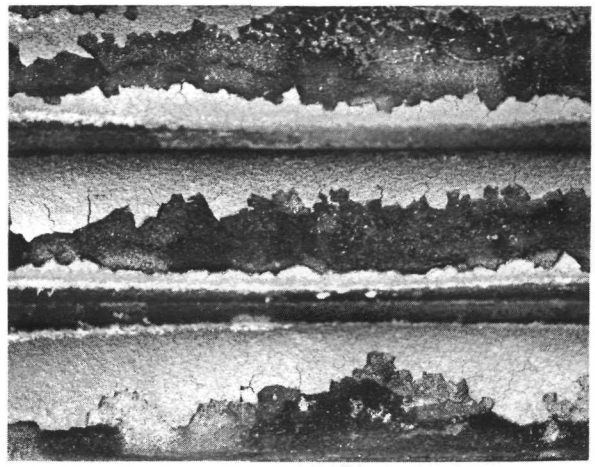

(a-2) Coating system sample 018-3-c (Mo sublayer - ZrO_2 outer layer).

(a) Face views of coating systems 017 and 018 after testing in hydrogen plasma for 30 minutes at $24.5X10^6$ W/m^2 (15 $Btu/(in.^2)(sec)$).

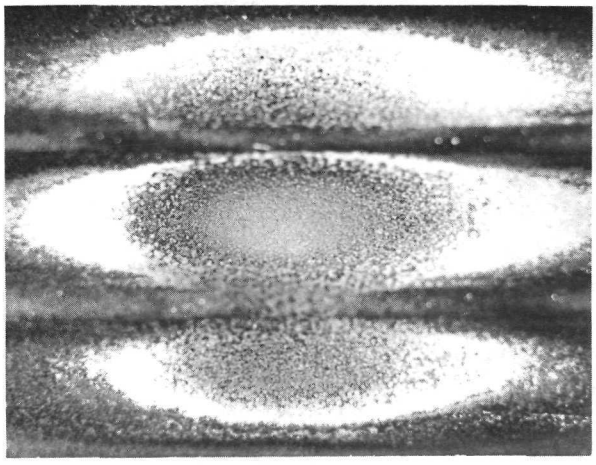

(b-1) Coating system sample 019-1-c (Mo sublayer - Y_2O_3 - stabilized ZrO_2 outer layer).

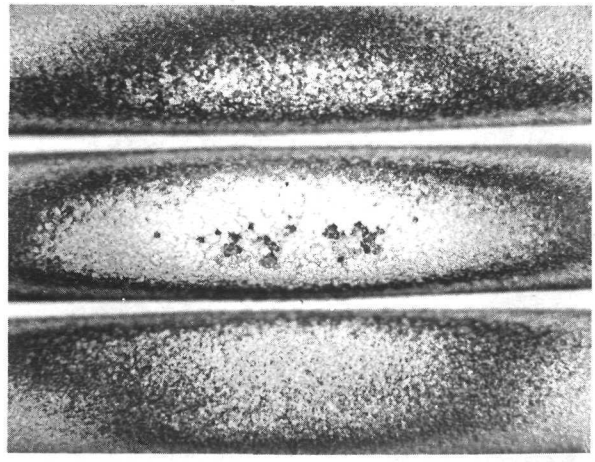

(b-2) Coating system sample 023-1-c (Mo sublayer - Y_2O_3 - stabilized ZrO_2 outer layer).

(b) Face views of coating systems 019 and 023 after testing in hydrogen plasma for 30 minutes at $24.5X10^6$ W/m^2 (15 $Btu/(in.^2)(sec)$).

Figure 17. - Structure effects on several simple coating systems of plasma testing. Original photographs, X3.

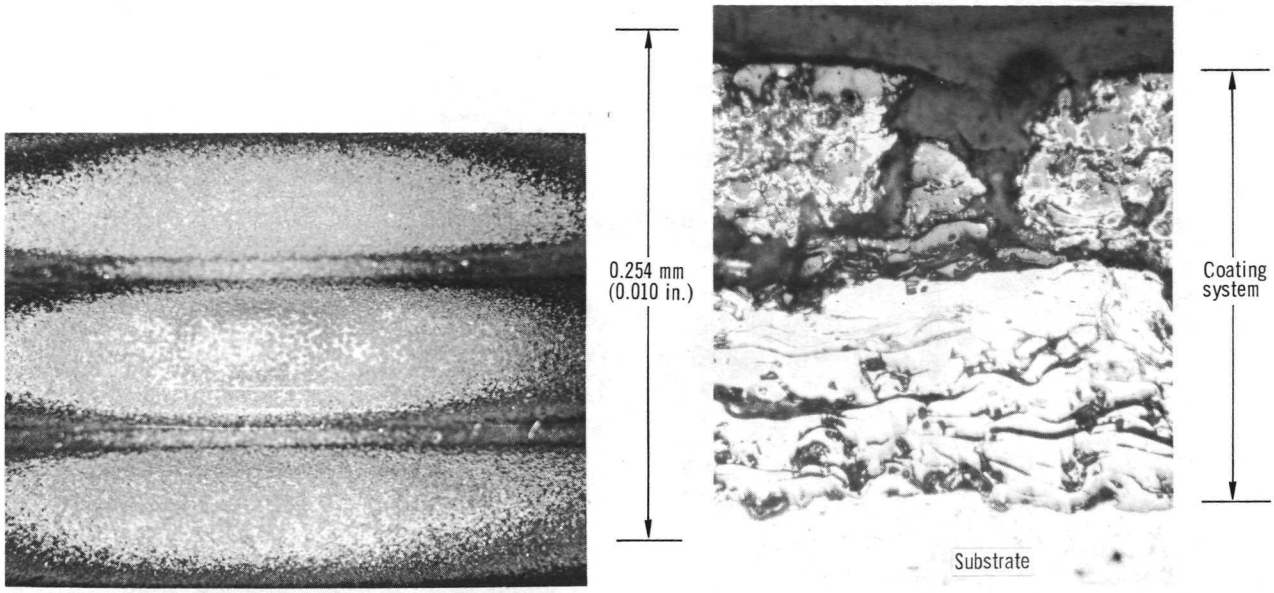

(a-1) Face view. Original photograph, X3.

(a-2) Section view. Original photomicrograph, X350.

(a) Views of coating system 005-1-c (Mo and nichrome sublayer - ZrO_2 outer layer) after testing in hydrogen plasma for 30 minutes at 24.5×10^6 W/m^2 (15 Btu/(in.^{2})(sec)).

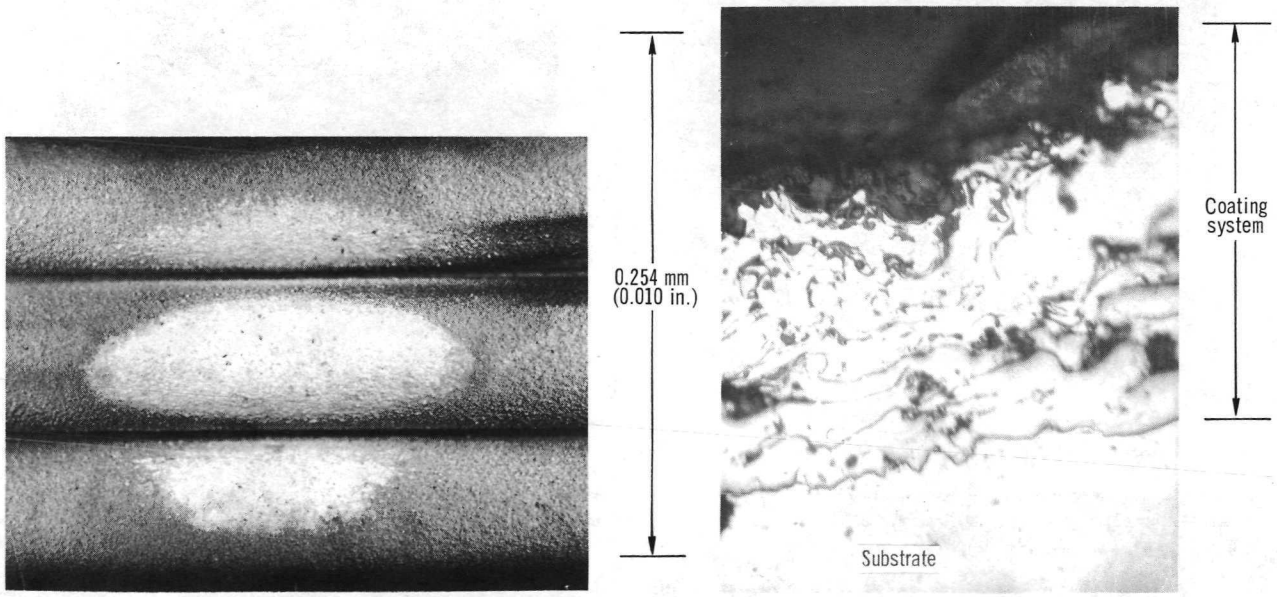

(b-1) Face view. Original photograph, X3.

(b-2) Section view. Original photomicrograph, X350.

(b) Views of coating system 004-2-c (Mo and nichrome sublayer - Al_2O_3 outer layer) after testing in oxygen mixed with hydrogen plasma for 30 minutes at 24.5×10^6 W/m^2 (15 Btu/(in.^{2})(sec)).

Figure 18. - Structure effects on layered coating systems of plasma testing.

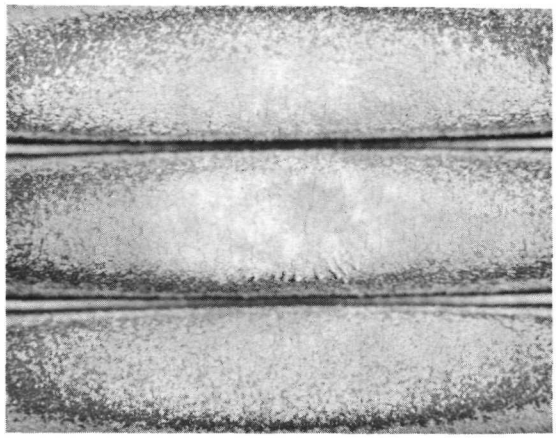

(a) Face view. Original photograph, X3.

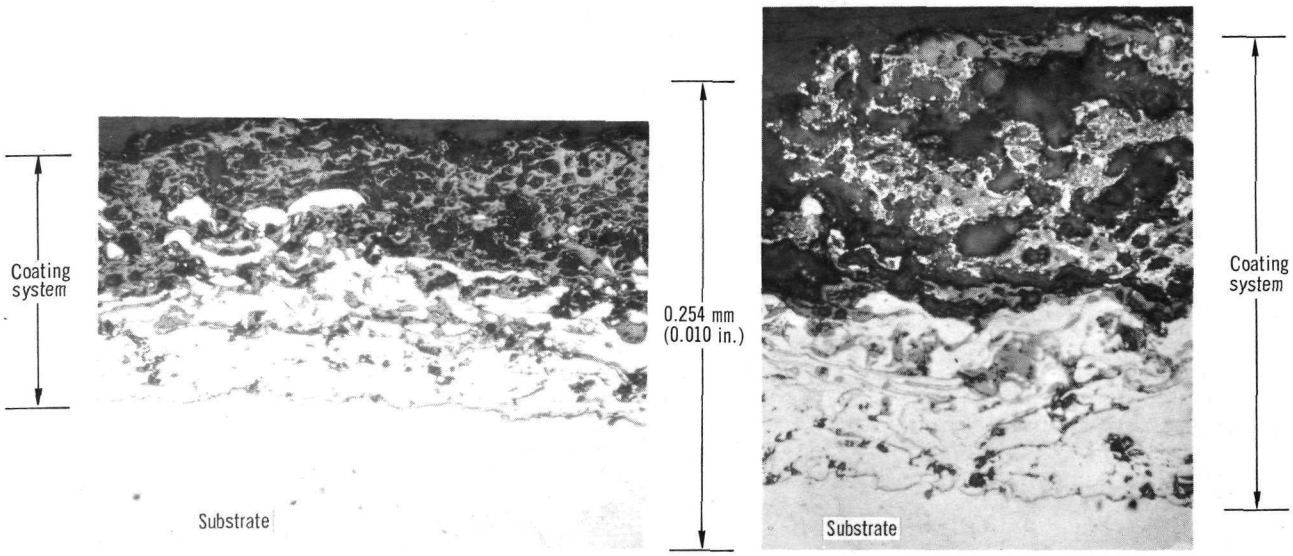

(b) Section view before testing. Original photomicrograph, X175.

(c) Section view after testing. Original photomicrograph, X350.

Figure 19. - Indications of probable sublayer melting in simple-graded coating system sample 001-1-c (Mo and nichrome/ZrO_2 sublayer - ZrO_2 outer layer) after testing in hydrogen plasma for 30 minutes at 24.5×10^6 W/m^2 (15 Btu/(in.^{2})(sec)).

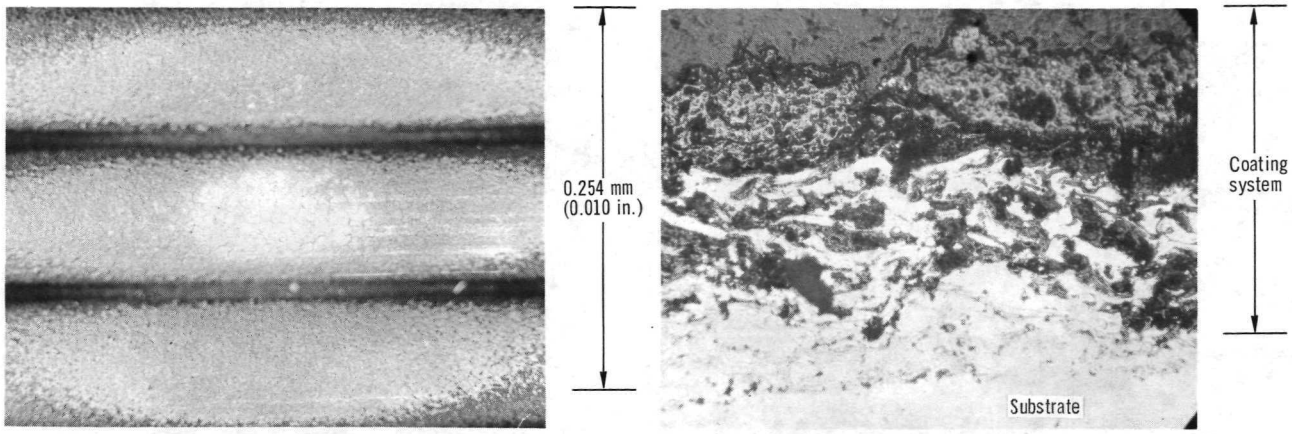

(a-1) Face view. Original photograph, X3.

(a-2) Section view. Original photomicrograph, X175.

(a) Views of coating system sample 007-1-c after testing in hydrogen plasma for 30 minutes at 24.5×10^6 W/m^2 (15 Btu/(in.^{2})(sec)).

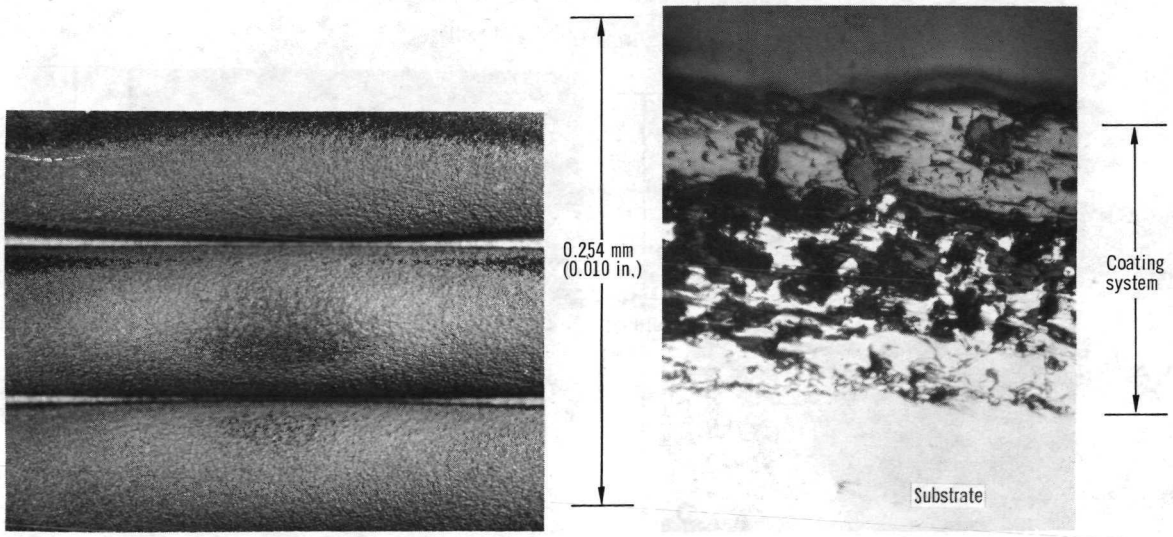

(b-1) Face view. Original photograph, X3.

(b-2) Section view. Original photomicrograph, X175.

(b) Views of coating system sample 007-1-c after testing in oxygen for 30 minutes at 24.5×10^6 W/m^2 (15 Btu/(in.^{2})(sec)).

Figure 20. - Structure effects on simple-graded coating system 007 (nichrome-nichrome/Al_2O_3 sublayer - ZrO_2 outer layer) of plasma testing.

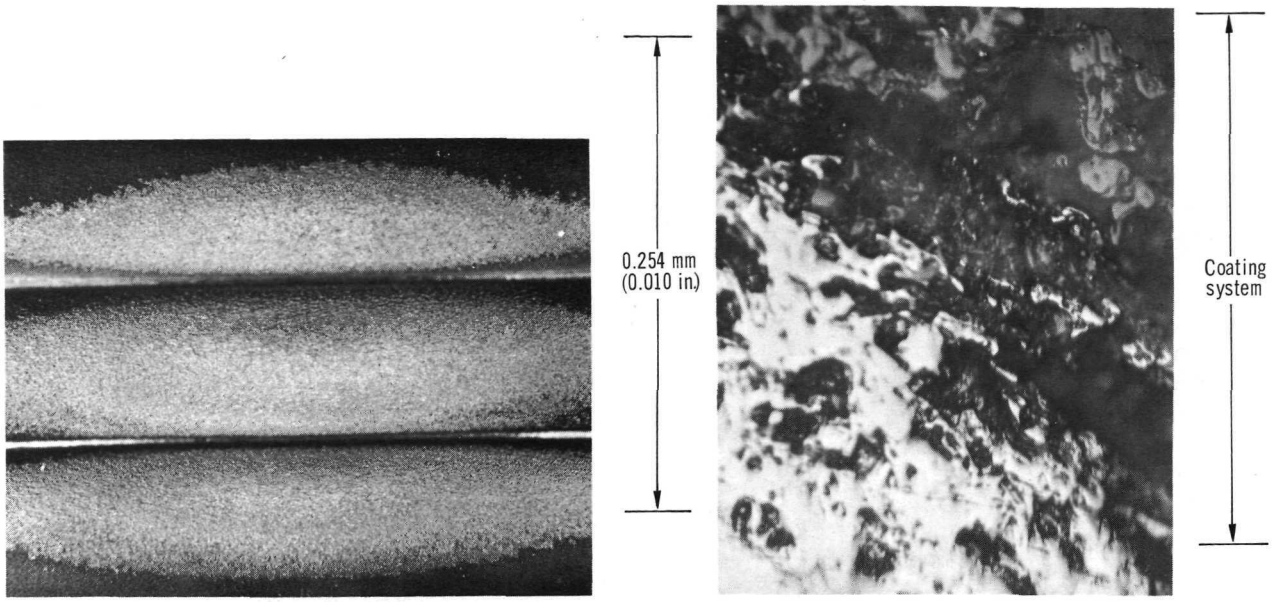

(a-1) Face view. Original photograph, X3.

(a-2) Section view. Original photomicrograph, X350.

(a) Views of coating system sample 002-1-c after testing.

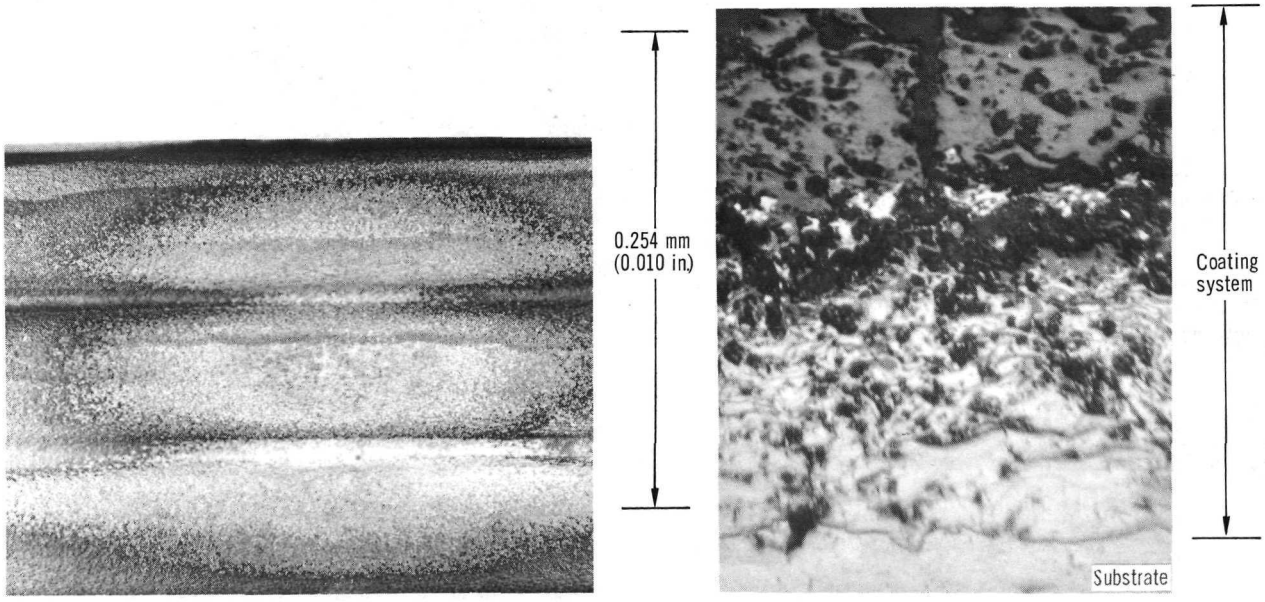

(b-1) Face view. Original photograph, X3.

(b-2) Section view. Original photomicrograph, X175.

(b) Views of coating system sample 020-2-c after testing.

Figure 21. - Structure effects on compound-graded coating systems 002 and 020 of testing in oxygen mixed with hydrogen plasma for 30 minutes at 24.5×10^6 W m^2 (15 Btu/($in.^2$)(sec)). Both systems are basically Mo/ZrO_2 sublayer - ZrO_2 outer layer .

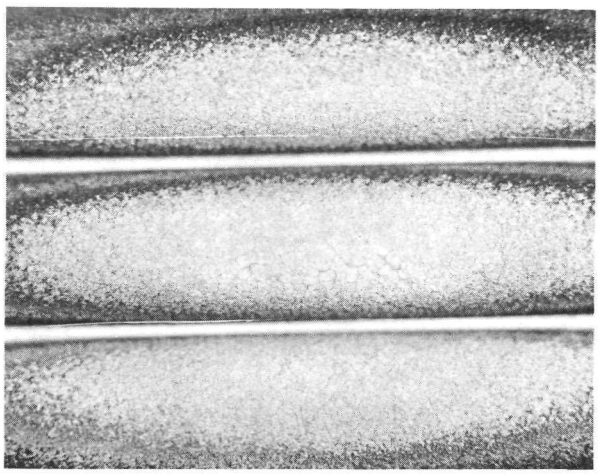

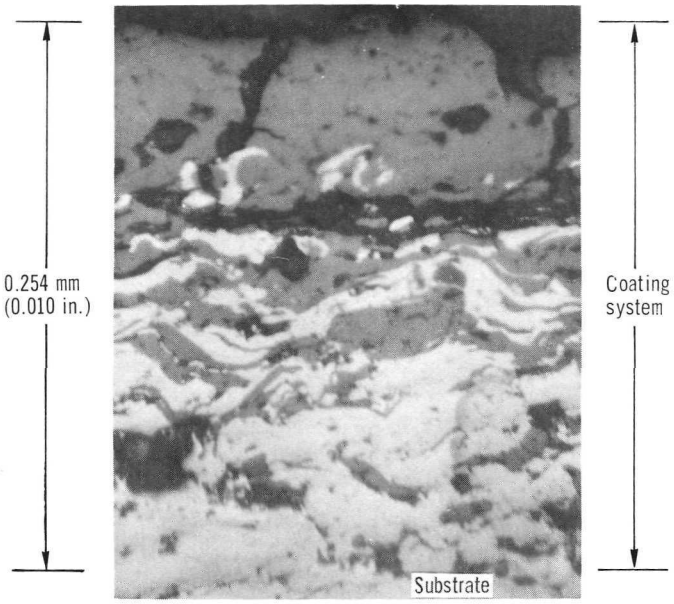

(a-1) Face view. Original photograph, X3.

(a-2) Section view. Original photomicrograph, X350.

(a) Views of coating system sample 002-1-c after testing in hydrogen plasma for 30 minutes at 24.5×10^6 W/m^2 (15 Btu/(in.^{2})(sec)).

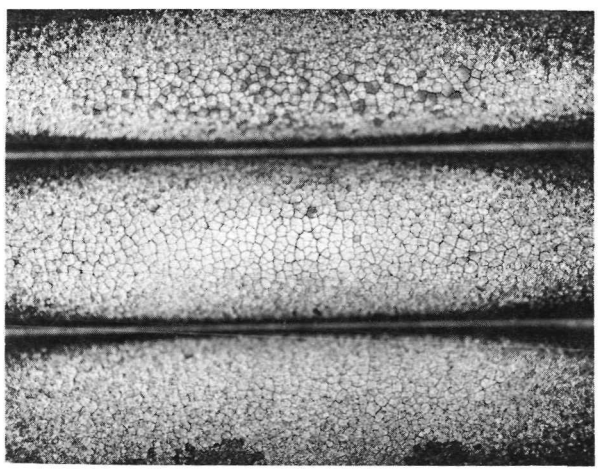

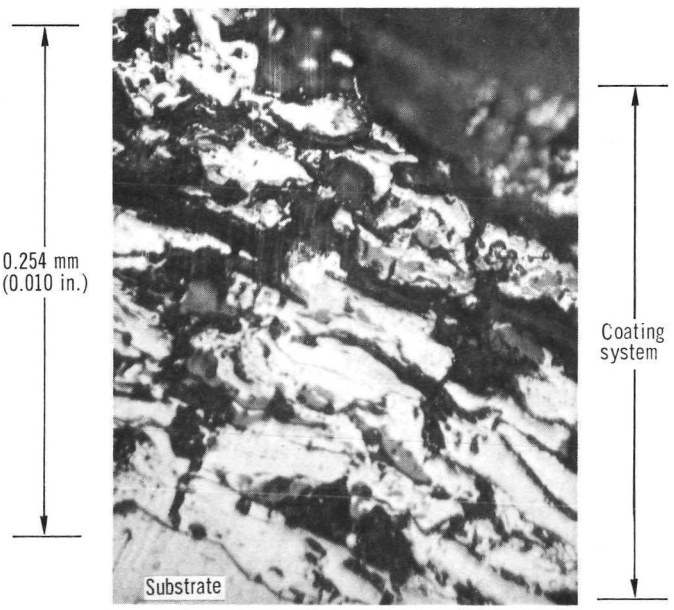

(b-1) Face view. Original photograph, X3.

(b-2) Section view. Original photomicrograph, X350.

(b) Views of coating system sample 002-3-c after testing in hydrogen plasma for 10 hours at 16.34×10^6 W/m^2 10 Btu/(in.^{2})(sec)).

Figure 22. - Structure effects on compound-graded coating system 002 (Mo-Mo/ZrO_2 + HfO_2 outer layer) of plasma testing.

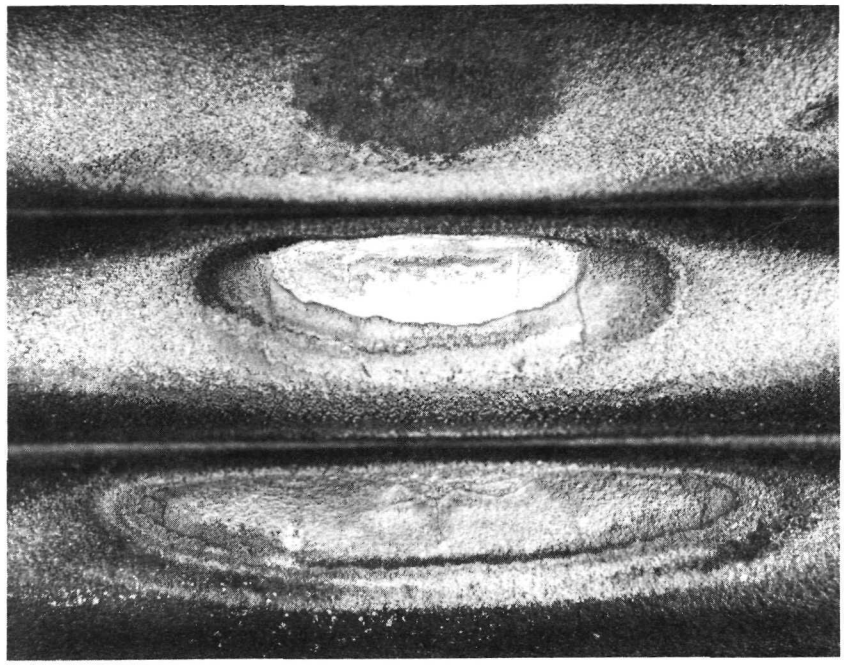

(a) Face view of coating system sample 006-2-c (tungsten + Nicoro 80 sublayer - tungsten + ZrO_2 + Cr outer layer) after testing.

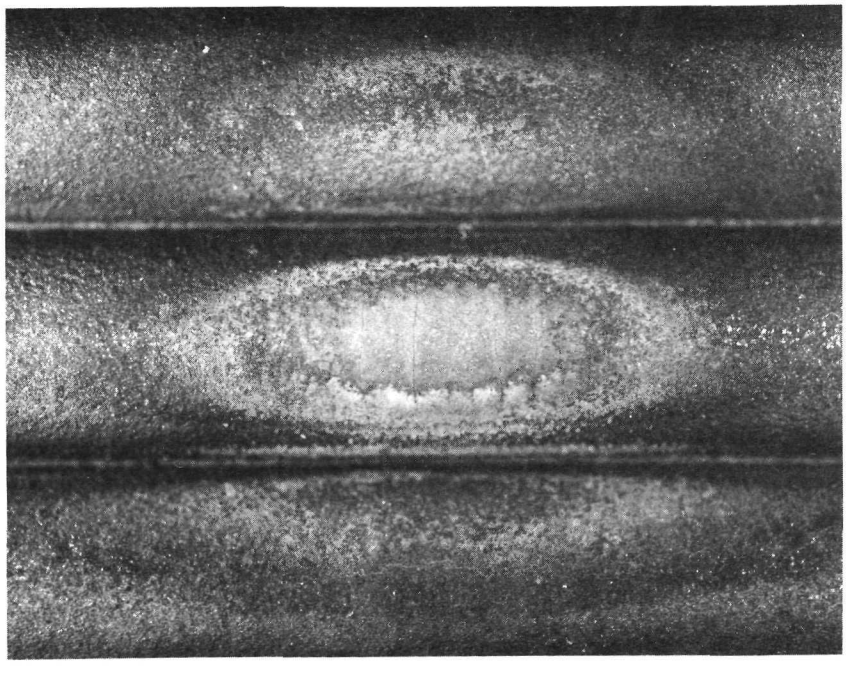

(b) Face view of coating system sample 008-2-c (Cr + Ni + Cr_2O_3 sublayer - Cr_2O_3 outer layer) after testing.

Figure 23. - Structure effects on two compound-graded coating systems of testing in oxygen mixed with hydrogen plasma for 30 minutes at 24.5×10^6 W/m^2 (15 Btu/(in.^{2})(sec)). Original photographs, X3.

NATIONAL AERONAUTICS AND SPACE ADMINISTRATION
WASHINGTON, D.C. 20546

OFFICIAL BUSINESS
PENALTY FOR PRIVATE USE $300

SPECIAL FOURTH-CLASS RATE BOOK

POSTAGE AND FEES PAID
NATIONAL AERONAUTICS AND SPACE ADMINISTRATION
451

U.S.MAIL

POSTMASTER: If Undeliverable (Section 158 Postal Manual) Do Not Return

"The aeronautical and space activities of the United States shall be conducted so as to contribute . . . to the expansion of human knowledge of phenomena in the atmosphere and space. The Administration shall provide for the widest practicable and appropriate dissemination of information concerning its activities and the results thereof."

—NATIONAL AERONAUTICS AND SPACE ACT OF 1958

NASA SCIENTIFIC AND TECHNICAL PUBLICATIONS

TECHNICAL REPORTS: Scientific and technical information considered important, complete, and a lasting contribution to existing knowledge.

TECHNICAL NOTES: Information less broad in scope but nevertheless of importance as a contribution to existing knowledge.

TECHNICAL MEMORANDUMS: Information receiving limited distribution because of preliminary data, security classification, or other reasons. Also includes conference proceedings with either limited or unlimited distribution.

CONTRACTOR REPORTS: Scientific and technical information generated under a NASA contract or grant and considered an important contribution to existing knowledge.

TECHNICAL TRANSLATIONS: Information published in a foreign language considered to merit NASA distribution in English.

SPECIAL PUBLICATIONS: Information derived from or of value to NASA activities. Publications include final reports of major projects, monographs, data compilations, handbooks, sourcebooks, and special bibliographies.

TECHNOLOGY UTILIZATION PUBLICATIONS: Information on technology used by NASA that may be of particular interest in commercial and other non-aerospace applications. Publications include Tech Briefs, Technology Utilization Reports and Technology Surveys.

Details on the availability of these publications may be obtained from:

SCIENTIFIC AND TECHNICAL INFORMATION OFFICE

NATIONAL AERONAUTICS AND SPACE ADMINISTRATION

Washington, D.C. 20546